https://doi.org/10.32685/pub.esp.37.2019.08
Published online 26 November 2020

Cenozoic Geologic Evolution of the Southern Tumaco Forearc Basin (SW Colombian Pacific)

Andrés PARDO–TRUJILLO[1]*, Sebastián ECHEVERRI[2], Carlos BORRERO[3], Alejandro ARENAS[4], Felipe VALLEJO[5], Raúl TREJOS[6], Ángelo PLATA[7], José–Abel FLORES[8], Agustín CARDONA[9], Sergio RESTREPO[10], Ángel BARBOSA[11], Hugo MURCIA[12], Carlos GIRALDO[13], Sergio CELIS[14], and Sergio A. LÓPEZ[15]

Abstract Tumaco is a forearc basin that contains insights into the Cenozoic geologic evolution of SW Colombia. In this region, the subduction of the Farallon and Nazca Plates beneath the South American Plate have controlled subsidence and magmatic activity during the Oligocene to recent times. A synthesis of seismic, stratigraphic, petrographic, geochronologic, and biostratigraphic data from outcrops and wells is presented. The Tumaco onshore basin has a trough–shaped symmetric geometry limited to the east by the Western Cordillera and to the west by the Remolino Grande–Gorgona Structural High. ca. 8000 m of sediments were accumulated in its depocenter during the Cenozoic. The sedimentites are composed of mudrocks, sandstones, and conglomerates, which vary in their proportions over time, and were mainly accumulated in open marine and deltaic environments. Calcareous nannofossils, foraminifera, and palynomorphs allowed assignment of the depositional time of the sedimentary units; however, the low abundance, preservation, and reworking of microfossils in some intervals require the use of multi–tools to determine the age of the deposits.

Sandstones are mainly litharenites and feldspathic litharenites, are texturally immature, and are composed of cherts fragments, basic to intermediate volcanic fragments, and crystals such as feldspars (Na and K), pyroxene, amphibole, and biotite, which can be associated with basic–intermediate volcanic, plutonic, and sedimentary rocks of the current basement of Western Cordillera. Sediment provenance analysis (detrital zircon and heavy minerals) suggests continuous volcanism from late Oligocene to Pleistocene times, the activity of which has increased since the middle Miocene. The presence of low percentages of pre–Cenozoic zircons and metamorphic rock fragments in the Miocene units are related to reworking of ancient sedimentary units or to a partial connection with the Central Cordillera basement. The study of Miocene – Pliocene outcrops and well cores allows the interpretation of a shallowing of the basin during the Messinian – Zanclean times. Volcanoclastic fans, as well as fluvial and coastal sediments, associated with the current Patía and Mira Rivers are partially covering the Miocene – Pliocene deposits.

Keywords: *Tumaco Basin, sedimentary provenance, biostratigraphy, Colombian Pacific, Cenozoic.*

Citation: Pardo–Trujillo, A., Echeverri, S., Borrero, C., Arenas, A., Vallejo, F., Trejos, R., Plata, Á., Flores, J.A., Cardona, A., Restrepo, S., Barbosa, Á., Murcia, H., Giraldo, C., Celis, S., & López, S.A. 2020. Cenozoic geologic evolution of the southern Tumaco Forearc Basin (SW Colombian Pacific). In: Gómez, J. & Mateus–Zabala, D. (editors), The Geology of Colombia, Volume 3 Paleogene – Neogene. Servicio Geológico Colombiano, Publicaciones Geológicas Especiales 37, p. 215–247. Bogotá. https://doi.org/10.32685/pub.esp.37.2019.08

1 andres.pardo@ucaldas.edu.co
Universidad de Caldas
Departamento de Ciencias Geológicas
Instituto de Investigaciones en Estratigrafía–IIES
Grupo de Investigación en Estratigrafía y Vulcanología–GIEV
Calle 65 n.° 26–10
Manizales, Colombia

2 sebastian.echeverri@usp.br
Universidad de Caldas
Instituto de Investigaciones en Estratigrafía–IIES
Grupo de Investigación en Estratigrafía y Vulcanología–GIEV
Calle 65 n.° 26–10
Manizales, Colombia

3 borrero_c@yahoo.com
Universidad de Caldas
Departamento de Ciencias Geológicas
Instituto de Investigaciones en Estratigrafía–IIES
Grupo de Investigación en Estratigrafía y Vulcanología–GIEV
Calle 65 n.° 26–10
Manizales, Colombia

4 alejandro.arenas@ucaldas.edu.co
Universidad de Caldas
Instituto de Investigaciones en Estratigrafía–IIES
Grupo de Investigación en Estratigrafía y Vulcanología–GIEV
Calle 65 n.° 26–10
Manizales, Colombia

5 diego.vallejo@ucaldas.edu.co
Universidad de Caldas
Instituto de Investigaciones en Estratigrafía–IIES
Grupo de Investigación en Estratigrafía y Vulcanología–GIEV
Calle 65 n.° 26–10
Manizales, Colombia

6 raul.trejos@ucaldas.edu.co
Universidad de Caldas
Instituto de Investigaciones en Estratigrafía–IIES
Grupo de Investigación en Estratigrafía y Vulcanología–GIEV
Calle 65 n.° 26–10
Manizales, Colombia

7 angeloplata@gmail.com
Universidad de Caldas
Instituto de Investigaciones en Estratigrafía–IIES
Grupo de Investigación en Estratigrafía y Vulcanología–GIEV
Calle 65 n.° 26–10
Manizales, Colombia

8 flores@usal.es
Universidad de Salamanca
Grupo de Geociencias Oceánicas

9 agcardonamo@unal.edu.co
Universidad Nacional de Colombia
Sede Medellín
Facultad de Minas
Medellín, Colombia

10 sarestrepom@unal.edu.co
Universidad Nacional de Colombia
Medellín, Colombia

11 dunito8@hotmail.com
Universidad de Caldas
Instituto de Investigaciones en Estratigrafía–IIES
Grupo de Investigación en Estratigrafía y Vulcanología–GIEV
Calle 65 n.° 26–10
Manizales, Colombia
University of Florida
Gainesville, USA

12 hugo.murcia@ucaldas.edu.co
Universidad de Caldas
Departamento de Ciencias Geológicas
Instituto de Investigaciones en Estratigrafía–IIES
Grupo de Investigación en Estratigrafía y Vulcanología–GIEV
Calle 65 n.° 26–10
Manizales, Colombia

13 klichegiraldo@gmail.com
Universidad de Caldas
Instituto de Investigaciones en Estratigrafía–IIES
Grupo de Investigación en Estratigrafía y Vulcanología–GIEV
Calle 65 n.° 26–10
Manizales, Colombia

14 sergio.celis@ucaldas.edu.co
Universidad de Caldas
Instituto de Investigaciones en Estratigrafía–IIES
Grupo de Investigación en Estratigrafía y Vulcanología–GIEV
Calle 65 n.° 26–10
Manizales, Colombia

15 seadlois@gmail.com
Agencia Nacional de Hidrocarburos

* Corresponding author

Resumen Tumaco es una cuenca de frente de arco que guarda información sobre la evolución geológica cenozoica del SW de Colombia. En esta región, la subducción de las placas de Farallón y de Nazca bajo la Placa de Suramérica ha controlado la subsidencia y actividad magmática durante el Oligoceno al reciente. Se presenta una síntesis de datos sísmicos, estratigráficos, petrográficos, geocronológicos y bioestratigráficos obtenidos a partir de afloramientos y pozos. La Cuenca Tumaco costa adentro tiene una geometría de artesa simétrica limitada al este por la cordillera Occidental y al oeste por el Alto Estructural Remolino Grande–Gorgona. Alrededor de 8000 m de sedimentos fueron acumulados en su depocentro durante el Cenozoico. Las sedimentitas corresponden a lodolitas, arenitas y conglomerados, que varían en su proporción a través del tiempo, y fueron principalmente acumuladas en ambientes marinos abiertos y deltaicos. Los nanofósiles calcáreos, foraminíferos y palinomorfos permitieron controlar la edad de acumulación de las unidades sedimentarias; sin embargo, debido a su baja abundancia y preservación y al retrabajamiento de microfósiles en algunos intervalos, se requiere el uso de herramientas múltiples para determinar la edad de los depósitos.

Las arenitas son principalmente litoarenitas y litoarenitas feldespáticas, texturalmente inmaduras y compuestas por fragmentos de chert, fragmentos volcánicos básicos a intermedios y cristales, tales como feldespato (Na y K), piroxeno, anfíbol y biotita, los cuales pueden asociarse con las rocas volcánicas básicas–intermedias, plutónicas y sedimentarias del actual basamento de la cordillera Occidental. El análisis de procedencia (circones detríticos y minerales densos) sugiere vulcanismo continuo desde el Oligoceno tardío al Pleistoceno, con incremento en la actividad desde el Mioceno medio. La presencia de bajos porcentajes de circones precenozoicos y fragmentos de rocas metamórficas en las unidades del Mioceno puede estar relacionada con el retrabajamiento de unidades sedimentarias antiguas o con una conexión parcial con el basamento de la cordillera Central. El estudio de afloramientos del Mioceno–Plioceno y núcleos de pozo permite interpretar una somerización de la cuenca durante el Mesiniano–Zancliano. Abanicos volcanoclásticos, así como sedimentos fluviales y costeros, asociados a los ríos Patía y Mira se encuentran cubriendo parcialmente los depósitos miocenos–pliocenos.

Palabras clave: *Cuenca Tumaco, procedencia sedimentaria, bioestratigrafía, Pacífico colombiano, Cenozoico.*

1. Introduction

The Tumaco Basin is part of a series of forearc basins located in the Pacific margin of the northern Andes (SW Colombia), where the Nazca and South American Plates have interacted at least since the Miocene (Aleman & Ramos, 2000; Barrero et al., 2007; Borrero et al., 2012; Hall & Wood, 1985; López–Ramos, 2009; Ramos, 1999). The basin axis has an ~N30°E orientation, which is parallel to the current arc system and the Colombian Pacific subduction zone (Figure 1). Tumaco Basin is divided by the Remolino Grande–Gorgona Structural High into onshore and offshore basins (Figure 1), also called the Manglares Basin by some authors (e.g., López–Ramos, 2009; Marcaillou & Collot, 2008). This region is characterized by a low relief and dense rain forest that has prevented the performance of systematic geological studies; thus, its geological history has remained poorly understood. The available geological maps are mainly based on geomorphology and scarce field and chronologic control (e.g., Nivia et al., 2003). In addition, most of the sedimentary deposits of the basin are below the surface. Therefore, the spatial and temporal relationships of the stratigraphic units are not well known. The presence of hydrocarbon shows within wells and outcrops indicates the existence of an active petroleum system (Barrero et al., 2007). Thus, oil exploration studies are the major source of information for the geology of the basin (e.g., López–Ramos, 2009; Suárez, 1990, 2007). Nevertheless, much of this information remains private and unpublished.

The basement of the Tumaco Basin is composed of Cretaceous basic igneous and sedimentary rocks, formed in the eastern Pacific and accreted to the continental margin of South America during the Late Cretaceous – Paleogene (Echeverri et al., 2015a; Spikings & Simpson, 2014; Villagómez et al., 2011). It is uncomfortably covered by siliciclastic and volcanoclastic rocks deposited from Eocene to Pliocene times (Barrero et al., 2007; Borrero et al., 2012; Echeverri, 2012; López–Ramos, 2009; Marín–Cerón & Sierra, 2011; Suárez, 1990, 2007). These Cenozoic rocks can reach more than 8000 m in the depocenter of the basin (Agencia Nacional de Hidrocarburos & Universi-

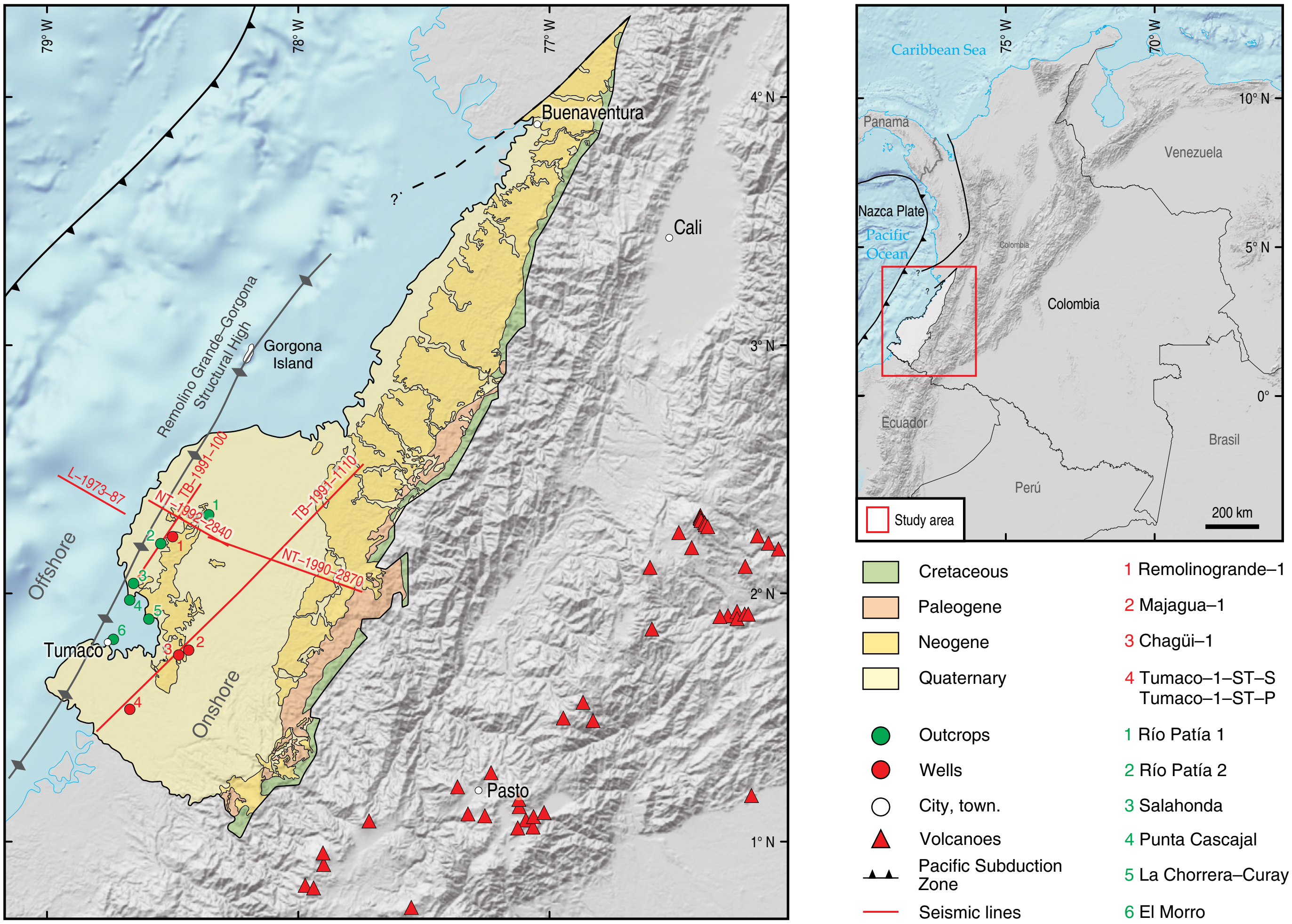

Figure 1. Location of the Tumaco Basin (yellow color) and studied localities mentioned in the text.

dad de Caldas, 2011a; Suárez, 1990, 2007). Neogene units are characterized by thick fluvial and deltaic siliciclastic deposits, which have been particularly considered for hydrocarbon explorations (Agencia Nacional de Hidrocarburos & Antek, 2013; Cediel et al., 2009; Echeverri, 2012; García, 2012; López–Ramos, 2009; Suárez, 1990, 2007).

Due to scarce information from the Pacific basins, in 2008, the Agencia Nacional de Hidrocarburos (ANH) initiated a campaign to drill wells in different sectors of these basins (e.g., ANH–Tumaco 1–ST–S and 1–ST–P wells and Buenaventura 1–ST–P) to investigate their petroleum systems. New geological information from wells and outcrops collected in recent multidisciplinary studies carried out by the Universidad de Caldas and the ANH (Agencia Nacional de Hidrocarburos & Universidad de Caldas, 2011a, 2011b) shed light on the geological history of the basin. A total of 1544 analyses were performed, including biostratigraphy (palynology, foraminifera, and calcareous nannofossils), petrography, and geochronology (U/Pb, Ar/Ar, and K/Ar methods). The integration of these results along with unpublished reports and published data (Bedoya et al., 2013; Borrero et al., 2012; Echeverri et al., 2015a, 2015b, 2016) allowed an age model to be established and the provenance and paleoenvironment for the sedimentary rocks of the basin to be illustrated.

2. Stratigraphy of the Tumaco Basin

Different stratigraphic nomenclatures have been proposed for the sedimentary rocks of the Tumaco Basin (Figure 2). Regional studies of the Servicio Geológico Colombiano (Arango & Ponce, 1980) used the stratigraphic model established by van der Hammen (1958), which was based on previous descriptions made by Oppenheim (1949). van der Hammen (1958) reported that the Guapi Formation (Pliocene) uncomfortably overlays the Miocene Naya Formation (Figure 2). Later, using mainly seismic and well information, Suárez (1990) proposed four lithostratigraphic units that have served as references for recent studies (e.g., Agencia Nacional de Hidrocarbuos & Universidad de Caldas, 2011a; Borrero et al., 2012; Escovar et al., 1992). This author compared the sedimentary record of the Tumaco Basin to the neighboring Borbón Basin in Ecuador, defining several units from base to top: (i) 1 Sur Unit Formation (Oligocene); (ii) Cayapas, Viche, and Angostura Formations (lower

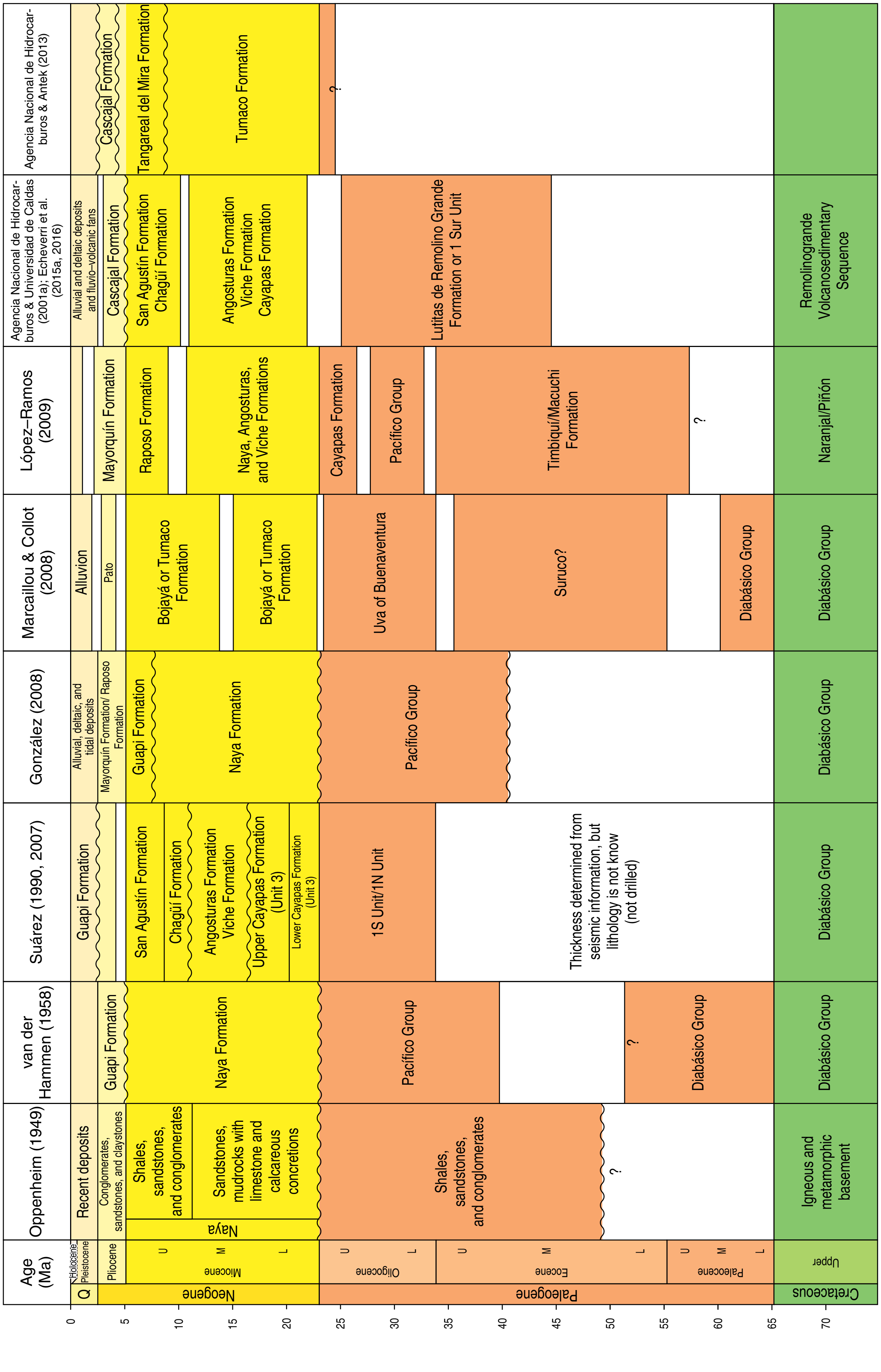

Figure 2. Chronostratigraphic chart showing the different stratigraphic nomenclatures employed for the Tumaco Basin.

– middle Miocene); (iii) Chagüí and San Agustín Formations (middle/upper Miocene – lower Pliocene); and (iv) Guapi Formation (Pliocene). Subsequently, Nivia et al. (2003) separated the youngest alluvial and deltaic deposits from the Guapi Formation, defining as Cascajal and Curay Members those underlying Pliocene and Miocene sedimentary deposits in the Nariño Department. Echeverri et al. (2016) proposed the term Cascajal Formation for the volcanoclastic rocks of the Messinian – Zanclean age reported by Nivia et al. (2003) (Figure 2). In contrast, in the northern part of the Tumaco Basin, Aspden (1984) and Aspden & Nivia (1985) proposed to divide the Neogene sedimentary cover into two formations: (i) Mayorquín Formation, composed mainly of mudrocks, and (ii) Raposo Formation, with conglomerates and sandstones. The stratigraphic and chronostratigraphic relationships of these units are unclear due to the low–biostratigraphic resolution and the absence of continuous outcrops. This has caused difficulties in performing regional correlations between southern and northern units (González, 2008; Instituto Colombiano de Geología y Minería & Instituto Geográfico Agustín Codazzi, 2005; López–Ramos, 2009; Nivia et al., 2003). Although Borrero et al. (2012) followed the stratigraphic nomenclature proposed by Suárez (1990), they grouped the sedimentary record into two megasequences, the Oligocene – middle Miocene sedimentary megasequence and the late Miocene – Holocene volcaniclastic megasequence. Finally, Agencia Nacional de Hidrocarburos & Antek (2013) informally proposed the names Tumaco and Tangareal del Mira Formations for upper Oligocene and Neogene deltaic deposits associated with the paleo–Patía and Mira Rivers (Figure 2). In this chapter, we will use the nomenclature of Borrero et al. (2012), Echeverri et al. (2011), and Echeverri et al. (2016).

3. Materials and Methods

3.1. Stratigraphy and Seismic Data

The stratigraphic information was obtained from electrical logs, ditch cutting, and core samples from the Remolino Grande–1 (total depth (TD) 9080'–2767 m), Majagua–1 (TD 14 280'–4352 m), and Tumaco 1–ST–S (TD 1899.6'–579 m) wells. This information was also integrated with data from outcrops located in the Tumaco Bay (e.g., Echeverri et al., 2016), with previous results reported by Suárez (1990) and López–Ramos (2009) and data from the ANH Tumaco 1–ST–P well (Agencia Nacional de Hidrocarburos & Antek, 2013). The well cores and cuttings are stored at the national core repository of Colombia (Litoteca Nacional, Piedecuesta, Santander).

Two regional seismic profiles were analyzed (Figure 3): (i) Perpendicular to the basin (dip lines) and composed of three seismic lines and (ii) more or less parallel to the strike of the basin (strike lines) and composed of two seismic lines (Figures 1, 3). These data were processed with GeoGraphix, where the main seismic reflectors and structures were identified (e.g., faults, folds, onlaps, toplaps, progradations). These reflectors were tied with the stratigraphic information of the Remolino Grande–1, Majagua–1, and Tumaco 1–ST–P wells. Additionally, as far as possible, the reflectors were tied with the surface geology map of Gómez et al. (2015). Subsequently, five horizons that represent chronostratigraphic boundaries were identified: (i) Cretaceous/Paleogene, (ii) Paleogene/lower Miocene, (iii) lower/middle Miocene, (iv) middle/upper Miocene, and (v) upper Miocene – Pliocene. Lower Miocene includes the Aquitanian and Burdigalian Stages; the middle Miocene, the Langian – Serravalian; and the upper Miocene, the Tortonian – Messinian.

3.2. Biostratigraphy

Biostratigraphic interpretations are based on distribution patterns and semiquantitative analyses of calcareous nannofossils and planktonic foraminifera reported for Majagua–1, Remolino Grande–1, Tumaco 1–ST–S, and Tumaco 1–ST–P wells (Agencia Nacional de Hidrocarburos & Antek, 2013; Agencia Nacional de Hidrocarburos & Universidad de Caldas, 2011a; Robertson Research inc. & Empresa Colombiana de Petróleos, 1981a, 1981b). The quality of the microfossil record was evaluated, and a composite section was built in which assemblages and age–indicative taxa were indicated. Biostratigraphic models were constructed using the standard biozones proposed by Blow (1969) and Berggren et al. (1995) for planktonic foraminifera and by Martini (1971) and Okada & Bukry (1980) for calcareous nannofossils. The biochronology of calcareous microfossil events follows the integrated scales of Agnini et al. (2014), Backman et al. (2012), Lourens et al. (2004), Raffi et al. (2006), and Wade et al. (2011). Taxonomical and biostratigraphic information described by Aubry (2014, 2015), Kennett & Srinivasan (1983), and Perch–Nielsen (1985) were also considered in the biostratigraphic interpretations. Biochronology of calcareous microfossil events follows the integrated scales of Agnini et al. (2014), Backman et al. (2012), Lourens et al. (2004), Raffi et al. (2006), and Wade et al. (2011). Taxonomical and biostratigraphic information described by Aubry (2014, 2015), Kennett & Srinivasan (1983), and Perch–Nielsen (1985) were also considered in the biostratigraphic models.

Most micropaleontological results were obtained from cutting samples, which in some cases (e.g., Remolino Grande–1) were collected at very large spacing, making its biostratigraphic interpretation difficult. Nevertheless, by integrating both calcareous nannofossils and planktonic foraminifera, it was possible to constrain the age from most of the wells. To achieve a more accurate age model, some considerations were taken in account. (i) Since the examined wells are composed of cuttings and cores that showed very abundant reworked microfossils, biostratigraphic analyses did not include specimens whose oc-

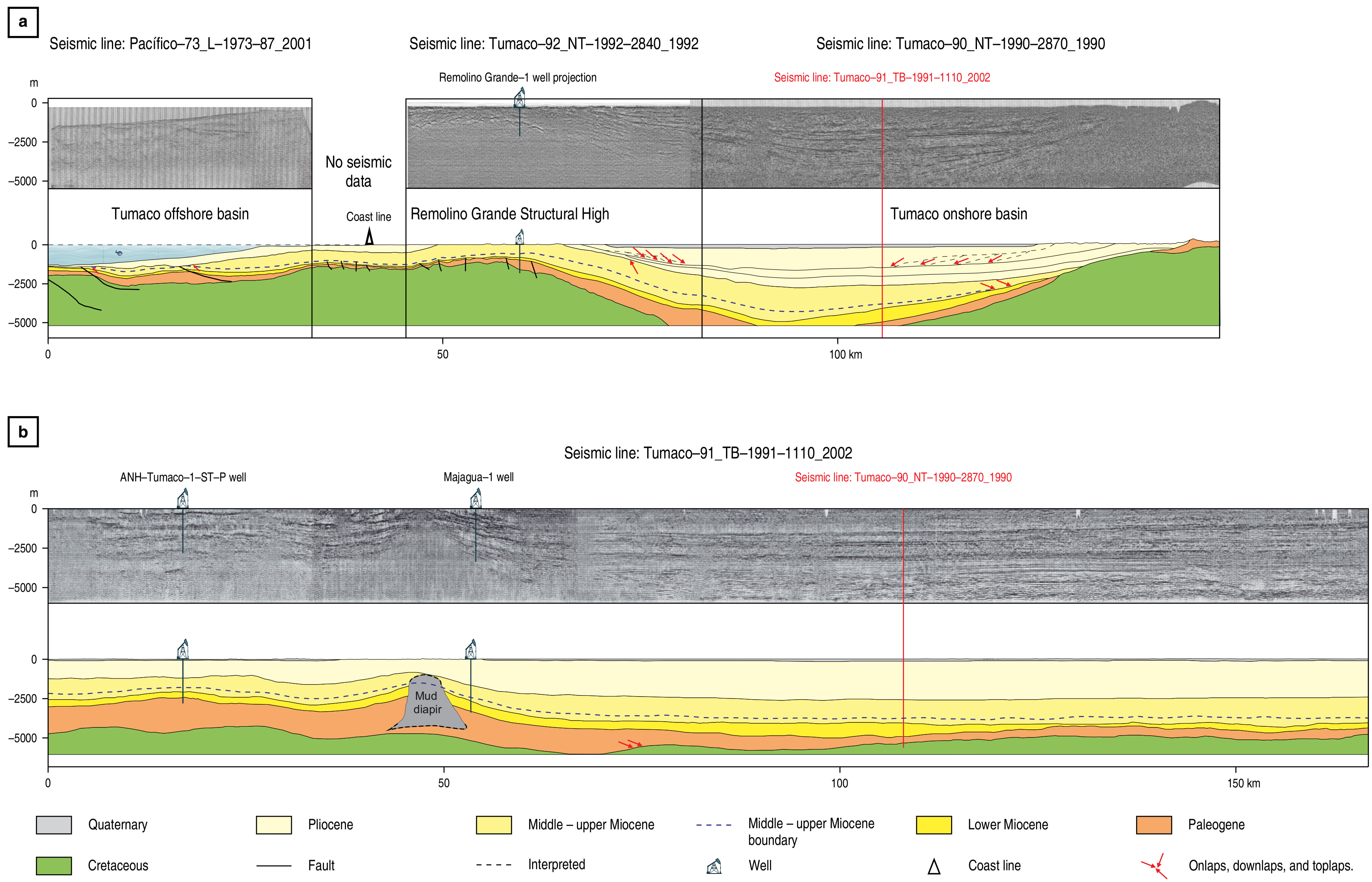

Figure 3. Geological cross–section of Tumaco, Western Cordillera, and Patía Basins based on seismic lines geologic mapping and well data. **(a)** Dip line. **(b)** Strike line. See Figure 1 for locations.

currence was very discontinuous or was observed in only one sample. (ii) Acmes or paracmes, which are regularly used as bioevents in studies of deep–sea sections, were not considered in our results. The fine–grained matrix regularly recorded in the material provokes a dilution, preventing the quantitative signal (Bedoya et al., 2013). (iii) Those stratigraphic intervals lacking biostratigraphic markers but bracketed by confirmed biozones were illustrated as intervals of indeterminate age because there was no micropaleontological support.

3.3. Sediment Provenance Analyses

A total of 30 grams of dried well cuttings was collected for petrographic analyses. This represents a 10–feet interval (3048 m) for the Majagua–1 well and intervals of 10', 20', and 30' for the Remolino Grande–1 well. Wet cutting samples were washed to remove contamination from the drilling process. Subsequently, a selection of very–fine sand to coarse–sand particles from cuttings was collected and mounted on glass slides and cover slips using balsam of Canada for petrographic analyses. A total of 82 thin sections were studied for petrography using ditch cutting samples: 26 from the well Remolino Grande–1, 38 from the well Majagua–1, and 18 from the well Chagüí–1. On average, 250 and 300 grains per slide were identified and counted. These data are represented in bar diagrams showing the relative percentages of the main components. Subsequently, the sandstones with a framework higher than 50% were selected to count their individual particles and to quantify the composition and are represented in Qt–F–L and Qm–F–Lt triangles of Folk (1974).

For heavy minerals and U/Pb geochronologic analyses, samples of ca. 1000 gr of dried cuttings were collected along tens to hundreds of feet and integrated in a single sample. The fraction > 63 < 250 μm was concentrated with sodium polytungstate (density of 2.89 g/cm^3) for heavy mineral analyses. In each sample, a thin section was made using a resin with a refraction index similar to balsam of Canada (1.539). A count of ca. 400 grains per slide was performed following the Ribbon–Counting method (Mange & Maurer, 1992). Mineralogical identification was based on Mange & Maurer (1992). The data obtained are represented in bar and triangular diagrams.

U/Pb geochronology was performed using the laser ablation inductively coupled plasma mass spectrometry (LA–ICPMS) method at a Washington State University Lab (USA). The samples were crushed and sieved (ca. 400–µm mesh). Zircon concentration was initially made following the gravitational methods on a Wifley table, passed through a Frantz magnetic separator and finally separated using methylene iodide. Approximately 100 grains per sample were analyzed in agreement with Gehrels et al. (2006). Separated zircons were mounted on an epoxy resin, manually polished and randomly studied. The maximum depositional U/Pb ages in detrital zircons were performed using the method described by Dickinson & Gehrels (2009). This age was acquired from the average of at least three grains of zircons with concordant ages (Kochelek et al., 2011). These results were plotted in relative probability diagrams using Isoplot 3.00 (Ludwing, 2003). ^{206}Pb/^{238}U ages were used for grains less than 1000 Ma, and ^{206}Pb/^{207}Pb ages were used for grains greater than 1000 Ma. Grains with more than 10% of discordance were not considered in the statistical analysis.

4. Results

The seismic lines show that the Tumaco onshore basin has a symmetric through shape limited to the E by the Western Cordillera and to the W by the Remolino Grande–Gorgona Structural High. Subhorizontal seismic reflectors indicate little deformation of the sedimentary sequence. However, in the southern sector of the basin, there is a structure at least 10 km wide that truncates the Paleogene and Neogene strata that has been interpreted as a mud diapir (Figure 3b; Cediel et al., 2009). In the depocenter, a thickness of 6805' (2074 m) is estimated for the Paleogene beds; 5713' (2546 m), for the lower – middle Miocene; and 11986 (3653.3 m), for the upper Miocene – Pliocene (Figure 3a, 3b). Calcareous microfossils are moderately to poorly preserved. Even though the sedimentary record was highly discontinuous, Majagua–1, Remolino Grande–1, and Tumaco 1–ST–P wells covered the largest stratigraphic record (Figures 4, 5). Calcareous microfossils suggest ages spanning from Bartonian (middle Eocene) in the Remolino Grande–1 well up to Pleistocene in the Tumaco 1–ST–P samples (Figures 4, 5). Miocene is the most common interval drilled by the wells, allowing the definition and correlation of different biostratigraphic intervals along the basin (Figures 4, 5). According to the biostratigraphic data in wells and seismic lines, the Tumaco Basin was divided into six chronostratigraphic sequences (Figure 3): (i) Upper Cretaceous, (ii) Paleogene (including Eocene and Oligocene beds), (iii) lower Miocene, (iv) middle Miocene, (v) upper Miocene – Pliocene, and (vi) Pliocene – Quaternary.

4.1. Upper Cretaceous

This series includes the volcano–sedimentary succession of Remolino Grande (Turonian – Campanian) (5630–9080'; 1716–2767 m) (Figure 3). This succession may be divided into two segments: (i) the lower segment, composed of mudrocks and fine sandstones interbedded with basalts and microgabbros, and (ii) the upper segment, formed by layers of basalts and microgabbros. Robertson Research inc. & Empresa Colombiana de Petróleos (1981b) provided a radiometric age in the interval 7250–7260' (2209–2212 m) of 82.2 ± 8.1 Ma (K/Ar in total rock). New Ar/Ar geochronological data (Agencia Nacional de Hidrocarburos & Universidad de Caldas, 2011a; Echeverri et al., 2015a) yield ages of 82.9 ± 4.8 Ma (6540–6550' or 1993–1996 m) and 76.2 ± 1.4 Ma (5680–5690', or 1731–1734 m) (Figure 4). These ages

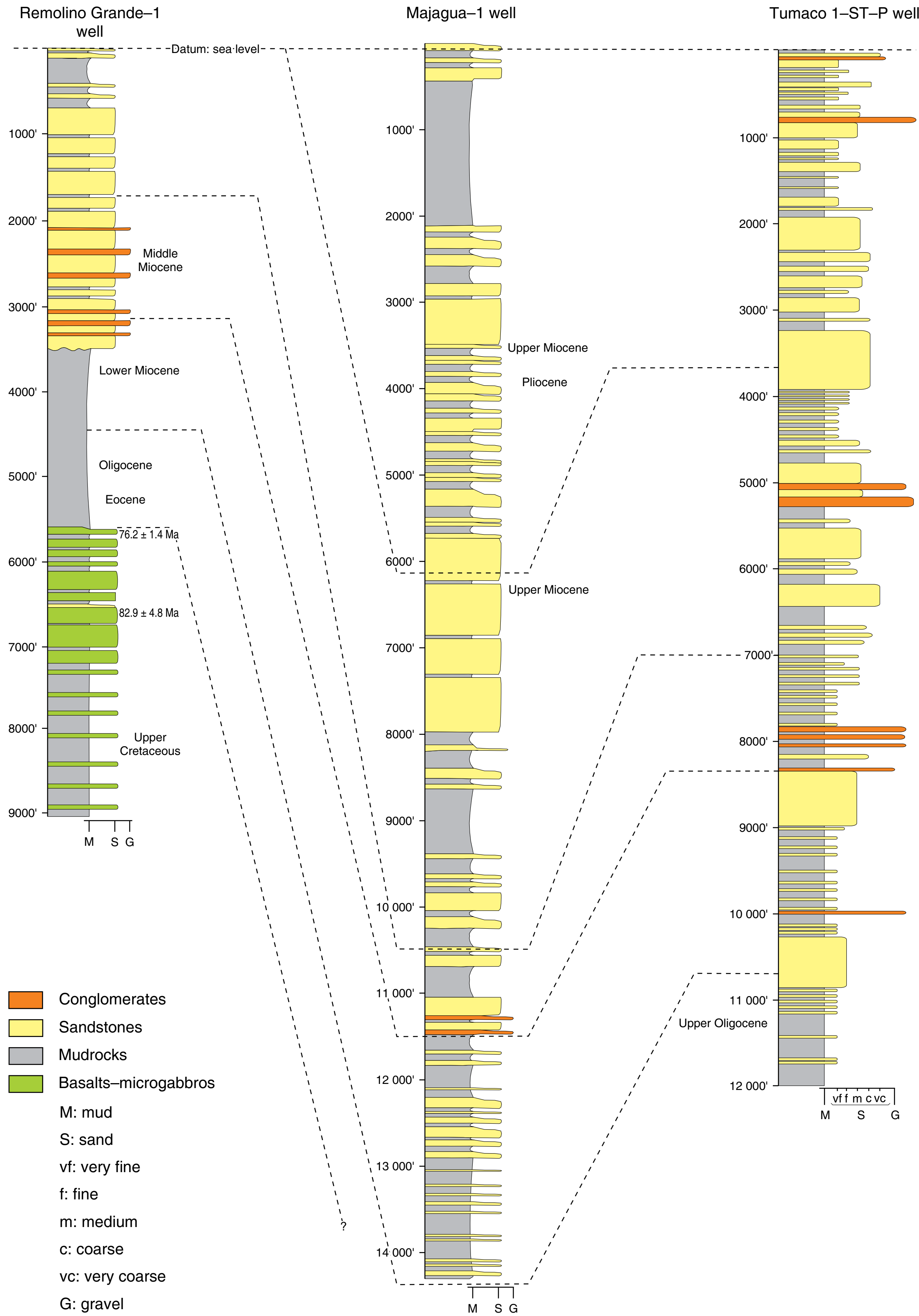

Figure 4. Chronostratigraphic correlation among the Remolino Grande–1, Majagua–1, and Tumaco 1–ST–P wells. Based on Agencia Nacional de Hidrocarburos & Universidad de Caldas (2011a) and Agencia Nacional de Hidrocarburos & Antek (2013).

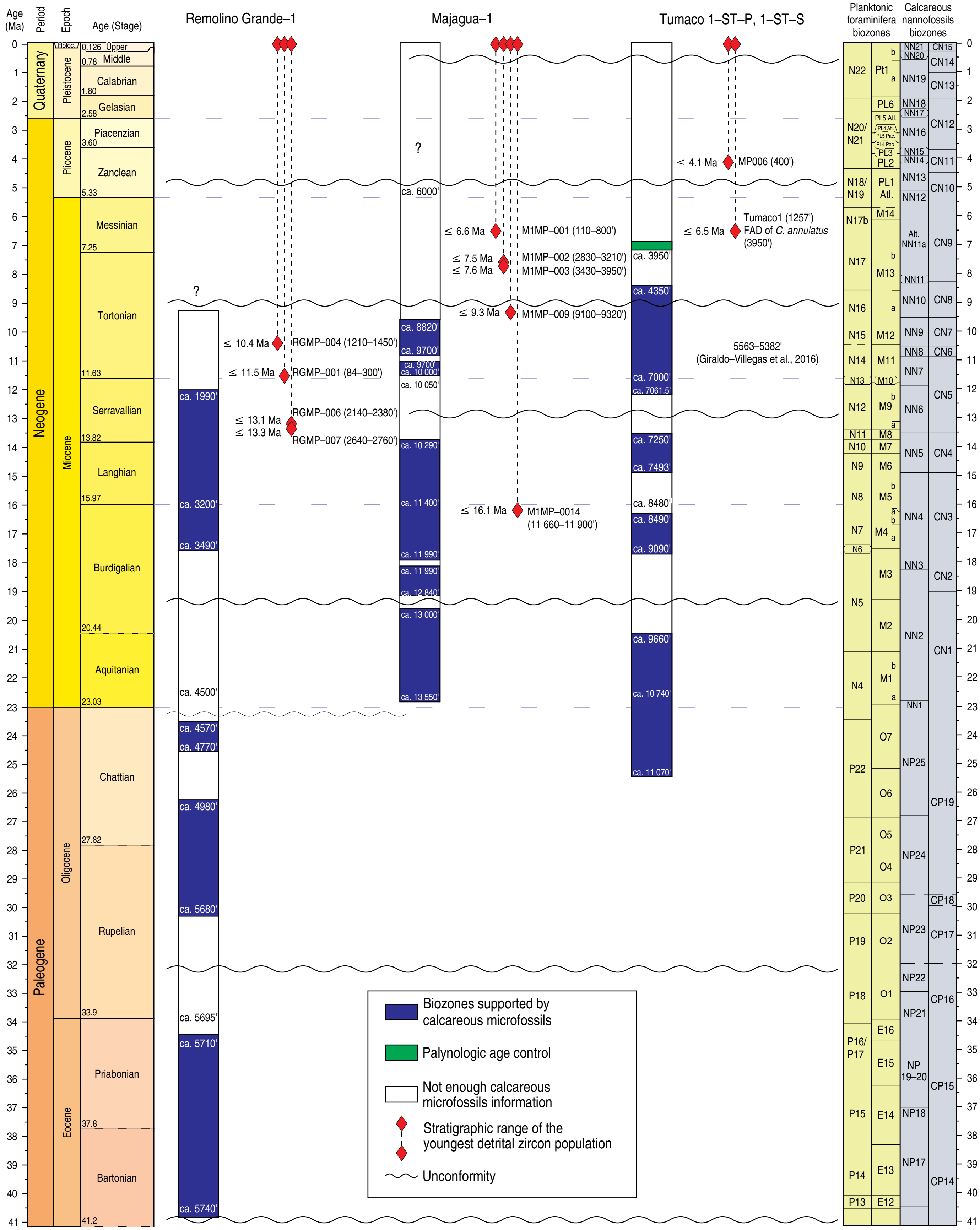

Figure 5. Ages of the Remolino Grande–1, Majagua–1, Tumaco 1–ST–P, and 1–ST–S wells based on calcareous microfossils, palynology, and detrital zircons. Geologic time scale based on Cohen et al. (2013; updated 2017/02).

can be correlated with the 98–60 Ma ages obtained from Gorgona Island by Serrano et al. (2011) and from the north of Ecuador by Vallejo et al. (2009). These rocks have been correlated by other authors with the Diabásico Group (sensu Nelson, 1962), the Volcánica Formation (sensu Aspden, 1984), and the Dagua/Piñón Formation (López–Ramos, 2009), located in the Western Cordillera of Colombia and Ecuador (Figure 2).

4.2. Paleogene

4.2.1. Seismic Lines

The Paleogene deposits were accumulated over a relatively smooth surface of the igneous Cretaceous basement. They onlap onto this basement to the east (Figure 3a). Paleogene deposits outcrop on the western border of the Western Cordillera (Figure 3a; Gómez et al., 2015). To the west, Paleogene reflectors can be identified over the Remolino Grande–Gorgona Structural High, where they become thinner and affected by normal faults. In the Tumaco offshore basin, Paleogene reflectors increase in thickness and are affected by thrust faults (Figure 3a). Paleogene deposits become thickened to the south of the basin, and their reflectors locally downlap the Cretaceous basement (Figure 3b).

4.2.2. Lithology

In the Remolino Grande–1 well, the Paleogene is mainly constituted by mudrocks and sandy siltstones interbedded with some sandstone beds (Figure 4). This unit can be correlated with the Lutitas de Remolino Grande Formation or 1 Sur Unit (Echeverri et al., 2015a; Suárez 1990, 2007), as well as the lower part of the Tumaco Formation of Agencia Nacional de Hidrocarburos & Antek (2013) (Figure 2). The Tumaco 1–ST–P well reached mudrocks, sublitharenites, and litharenites, interpreted as late Oligocene (Chattian) shelf–prodelta to delta front deposits. Benthic foraminifera such as *Osangularia* sp., *Gyroidinoides broeckhiana, Discorbinella* sp., *Anomalinoides cicatricose*, and *Anomalinoides semicribata* suggest sedimentation in the upper–middle part of the continental slope (Agencia Nacional de Hidrocarburos & Antek, 2013).

4.2.3. Biostratigraphy

The lowest sample with calcareous microfossil recovery in Remolino Grande–1 well yielded *Reticulofenestra bisecta, Reticulofenestra reticulata,* and Paleocene and Eocene reworked species (*Sphenolithus anarrhopus* and *Sphenolithus primus, Nannotetrina* spp.). The young assemblage suggests the biozones NP16 and NP19 (Bartonian – Priabonian; Agnini et al., 2014; Perch–Nielsen, 1985). For the Oligocene, diagnostic species of planktonic foraminifera were not identified; however, calcareous nannofossils such as *Cyclicargolithus abisectus, Sphenolithus ciperoensis*, and *Sphenolithus distentus* were recorded in some samples. Oligocene/Miocene boundary markers were not found at the Remolino Grande–1 well (Figure 5). Nevertheless, planktonic foraminifera bioevents such as the last occurrence of the *Paragloborotalia opima* at 27.30 Ma in the biozone O6 and the first occurrence of *Paragloborotalia kugleri* at 23.73 Ma in the biozone M1a according to Wade et al. (2011) support the Paleogene/Neogene boundary near 10 740' at the Tumaco 1–ST–P well (Figure 5). This interpretation indicates that Paleogene calcareous nannofossils reported in shallower levels correspond to reworked species. Due to the lack of diagnostic microfossils, this boundary was unclear in the Remolino Grande–1 well; therefore, it was placed at 4500' after seismic correlation with the Tumaco 1–ST–P well (Figures 3, 4, 5). Even though Paleocene deposits were not found in the Remolino Grande–1 well, lower Paleocene deposits have been recently reported in outcrops of the Gorgona Island 85 km to the NE (Bermúdez et al., 2016). In Figure 5, the correlation of the lower part of the Remolino Grande–1 and Tumaco 1–ST–P wells with the calcareous nannofossils and planktonic foraminifera standard zones is shown. This interval ranges between NP19–NP25 and P16–P22, respectively.

4.2.4. Petrography

In the Remolino Grande–1 well, two ditch cutting samples were used for petrographic analyses. They have abundant grains of sedimentary rocks (27–80 %, siltstones, sandy siltstones, and chert; Figure 6). Plagioclase, mono– and polycrystalline quartz, pyroxene, biotite, hornblende, glauconite, and opaque minerals are present in lower proportions. Some algae and foraminifera are observed. Sandstone grains were selected to know their framework composition. They were classified as poorly sorted subarkoses, with fine to coarse angular to subrounded grains. They are composed of monocrystalline (32–44 %) and polycrystalline (21–30 %) quartz, plagioclase (10–23 %), intermediate volcanic rocks (5–6 %), chert (4–15 %), biotite (1–2 %), muscovite (1%), and chlorite (3%). Mud matrix and calcareous cement are common.

4.2.5. Heavy Minerals

The analyzed samples present higher abundances of unstable compared to stable phases. Stable phases include zircon (2–7 %) and tourmaline (1%). Unstable phases correspond to apatite (4–25 %), clinopyroxene (10–52 %), orthopyroxene (1–12 %), hornblende (1–13 %), and minerals of the epidote group (25–40 %). Olivine, oxyhornblende, and biotite are present at 1% each. In the Tumaco 1–ST–P well, the samples contain mainly unstable phases with abundant amphibole, pyroxene and, in lower proportions, epidote, apatite, clinopyroxene, and orthopyroxene. In this interval, detrital zircons were not obtained.

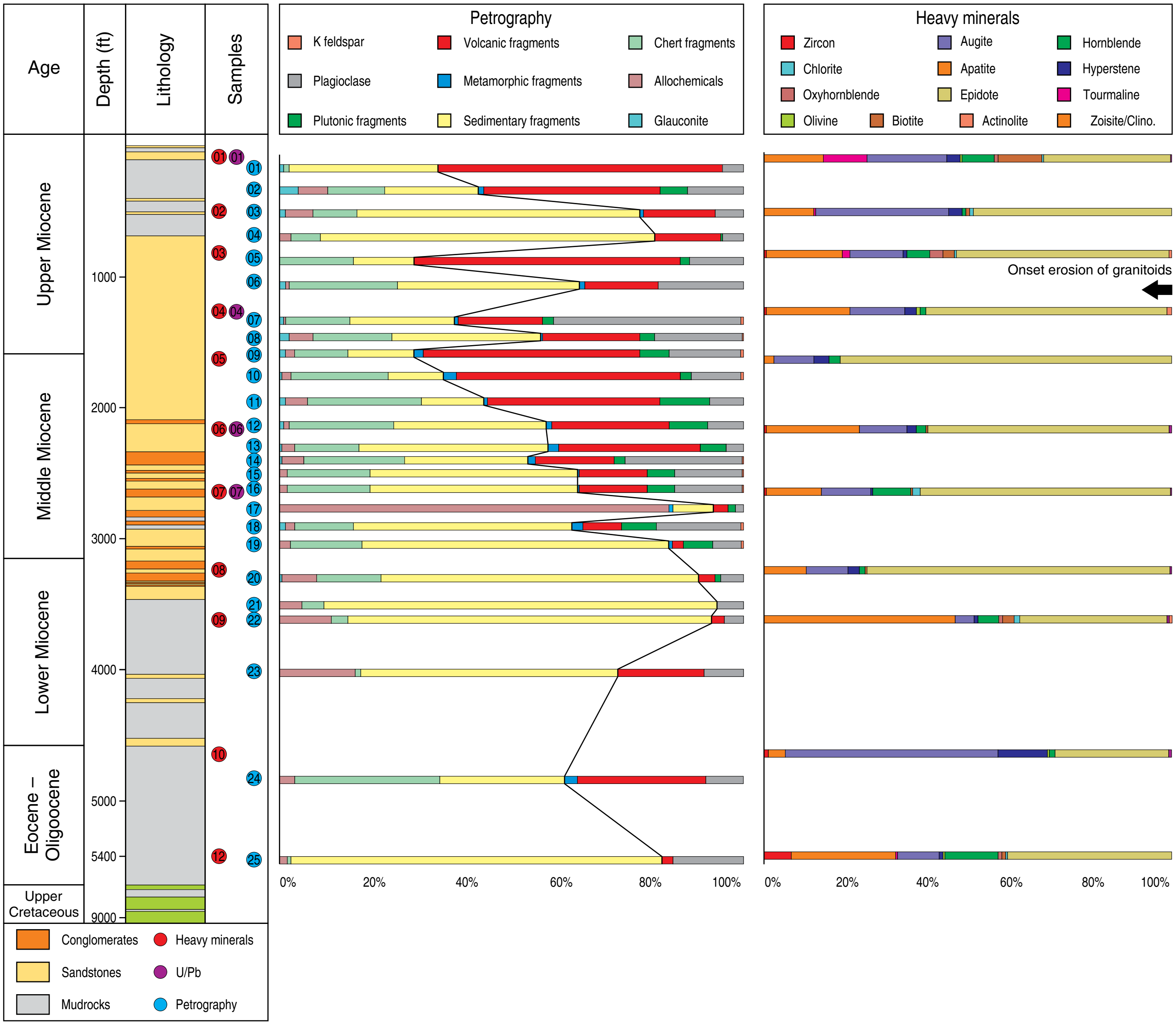

Figure 6. Stratigraphic log of the Remolino Grande–1 well, and bar diagrams representing the composition of the ditch cuttings and heavy minerals. Allochemicals include calcareous fossil remains (mainly foraminifera, bivalves, and gastropods).

4.3. Lower Miocene (Aquitanian – Burdigalian)

This interval has been identified in the Remolino Grande–1 (3200–4500'), Majagua–1 (14280–11220), and Tumaco 1–ST–P (8480–10740') wells.

4.3.1. Seismic Lines

The lower Miocene reflectors onlap onto the Paleogene deposits towards the E of the basin (Figure 3a). Westward, they become thinner and pinch–out in the Remolino Grande–Gorgona Structural High. In the offshore Tumaco Basin, the lower Miocene reflectors are concordant with Paleogene and middle Miocene reflectors and seem to be in toplap against the Pliocene reflectors in the westernmost part of the seismic line (Figure 3a). In the Remolino Grande–Gorgona Structural High, the lower Miocene beds seem to fill some valleys dissected in the Paleogene deposits. In the strike line, the lower Miocene reflectors become thinner to the north, but they are concordant with the Paleogene and middle Miocene sequences.

4.3.2. Lithology

In the Remolino Grande–1 well, there is a dominance of claystones and sandy siltstones interbedded with some sandstone beds, which change abruptly to conglomerates and sandstones in the upper part of the succession (Figure 4). This interval has abundant fossils of bivalves, gastropods, foraminifera, and carbonized organic matter. In the Majagua–1 well, lower Miocene deposits are composed of mudrocks interbedded with fine–medium sandstones and sandy mudstones. Foraminifera and mollusk shells are abundant. In the Tumaco 1–ST–P, the rocks of this period are characterized by an alternation of highly bioturbated mudrocks, massive and laminated sublitharenites, feldspathic litharenites, litharenites, and some beds of polymictic conglomerates. Paleontological content includes shark teeth (Agencia Nacional de Hidrocarburos & Antek, 2013).

4.3.3. Biostratigraphy

Calcareous nannofossil events are the most efficient biostratigraphic indicator at the Tumaco 1–ST–P and Majagua–1 wells in the lower Miocene deposits. The appearances of *Discoaster druggi, Heliscoaphaera ampliaperta*, and *Sphenolithus heteromorphus* and the extinction of *Triquetrorhabdulus carinatus* in these wells mark the beginning of the Miocene (Aubry, 2014, 2015; Backman et al., 2012; Perch–Nielsen, 1985). This is in agreement with the recovery of the short–lived *Sphenolithus belemnos* in the Majagua–1 well. For this interval, the Remolino Grande–1 well is characterized by the last occurrence of *H. ampliaperta* and *S. heteromorphus* and the occurrence of *Globigerinoides diminutus*, whose biostratigraphic range is described for the late Burdigalian – Langhian (Aubry, 2014; Backman et al., 2012; Kennett & Srinivasan, 1983). This indicates that Remolino Grande–1 encompasses a long–lasting gap (ca. 5 Ma), which includes the Aquitanian and the lower–middle part of the Burdigalian. In Figure 5, the stratigraphic equivalence of the Remolino Grande–1, Majagua–1, and Tumaco 1–ST–P wells with the calcareous nannofossils and planktonic foraminifera standard zones is represented. This portion represents an interval between NN2 to NN6 and N4 to N12, respectively.

4.3.4. Petrography

The ditch cutting samples from the Majagua–1 and Remolino Grande–1 wells are composed mainly of sedimentary rocks (56–90 %; mudrocks, cherts, calcite, sandy shales, sandstones) and, in lower proportions, plagioclase, volcanic and plutonic lithics. Fragments of quartz (mono– and polycrystalline), biotite, hornblende, pyroxene, glauconite, and bioclasts (foraminifera, algae, echinoderms) occur in lower proportions.

The sandstone grains of the Majagua–1 (Figure 7) and Remolino Grande–1 wells were selected to study the composition of their framework. They are classified as feldspathic litharenites and arkoses (Figures 8, 9). The sandstones are poorly sorted, fine to medium size, with rounded to subangular grains. They have a high content of plagioclase (34–68 %), with lower proportions of quartz (3–32 % monocrystalline and 2–21 % polycrystalline) and lithic fragments (1–39 %). Lithic fragments are mainly volcanic of intermediate composition (6–39 %), chert (2–15 %), and low proportions of plutonic rocks, sandstones, micaceous and graphitic schists (≤ 1%) (Figures 7, 9). The accessory minerals are composed of hornblende (5%), epidote (2–3 %), glauconite (1%), biotite (1–3 %), chlorite (2–6 %), and muscovite (< 1%). In the Tumaco 1–ST–P well, the sandstones include litharenites and lithic greywackes, with angular fragments of sedimentary, volcanic, and metamorphic rocks (Agencia Nacional de Hidrocarburos & Antek, 2013).

4.3.5. Heavy Minerals

Two samples from the Remolino Grande–1 well and four from the Majagua–1 well were analyzed (Figures 6, 7, 10). In the Remolino Grande–1 well, stable phases are almost absent, with only 1% zircon. Unstable phases include apatite (47%), clinopyroxene (4–10 %), hornblende (2–5 %), and minerals of the epidote group (36–74 %). Oxyhornblende, actinolite, and chlorite are present in low proportions (≤ 1%). A higher proportion of unstable with respect to the ultrastable phases was found in the Majagua–1 well (Figures 7, 10). Ultrastable phases include zircon (4–26 %) and traces of tourmaline (≤ 1%). Unstable phases include apatite (51–75 %), minerals of the epidote group (1–12 %), biotite (2–4 %), clinopyroxene (2–10 %), ortopyroxene (≤ 1%), chlorite (≤ 2%), hornblende (≤ 2%), and traces of oxyhornblende and glauconite (Figures 7, 10). In the Tumaco 1–ST–P well, a greater proportion of unstable minerals compared to stable ones was also observed (Agencia Nacional de Hidrocarburos & Antek, 2013). Ultrastable phases include zircon and tourmaline (≤ 1%). Unstable phases include hornblende (31–56 %), minerals of the epidote group (1–41 %), apatite (< 1–3 %), clinopyroxene (6–28 %), biotite (≤ 3%), chlorite (1–2 %), sphene (≤ 1%), and garnet (< 1–4 %).

4.3.6. Detrital Geochronology

In the Majagua–1 well, the sample M1MP–014 (depth 11660–11900') was analyzed (Figure 11). A maximum depositional age of 16.1 Ma (Burdigalian) was found. This sample shows four main zircon populations: (i) 18.9 Ma, (ii) 45.0 Ma, (iii) 51.3 Ma, and (iv) 20.7 Ma. Oligocene (28.6 Ma), Late Cretaceous (68.6 Ma, 74.4 Ma, 74.9 Ma, 74.9 Ma, 76.9 Ma, and 83.2 Ma), and Precambrian (556.7 Ma, 557.4 Ma, 844.4 Ma, and 1657.0 Ma) zircons are present, but they are not abundant enough to form a population.

4.4. Middle Miocene (Langhian – Serravallian)

Rocks of this period were identified in the Remolino Grande–1 (1450–3200'), Majagua–1 (10500–11400'), and Tumaco 1–ST–P (7000–8480') wells.

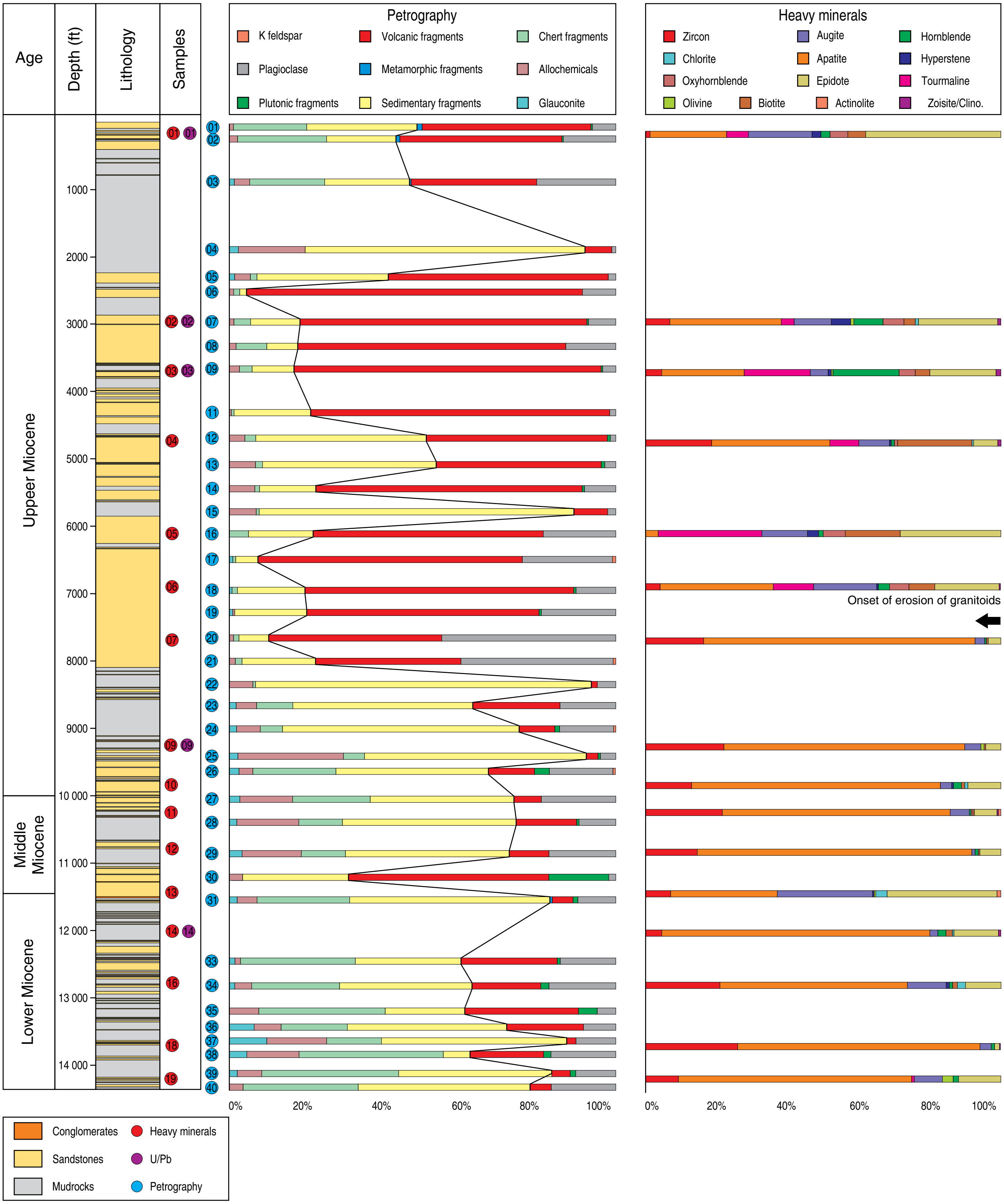

Figure 7. Stratigraphic log of the Majagua–1 well, and bar diagrams representing the composition of the dish cuttings and heavy minerals. Allochemicals include calcareous fossil remains (mainly foraminifera, bivalves, and gastropods).

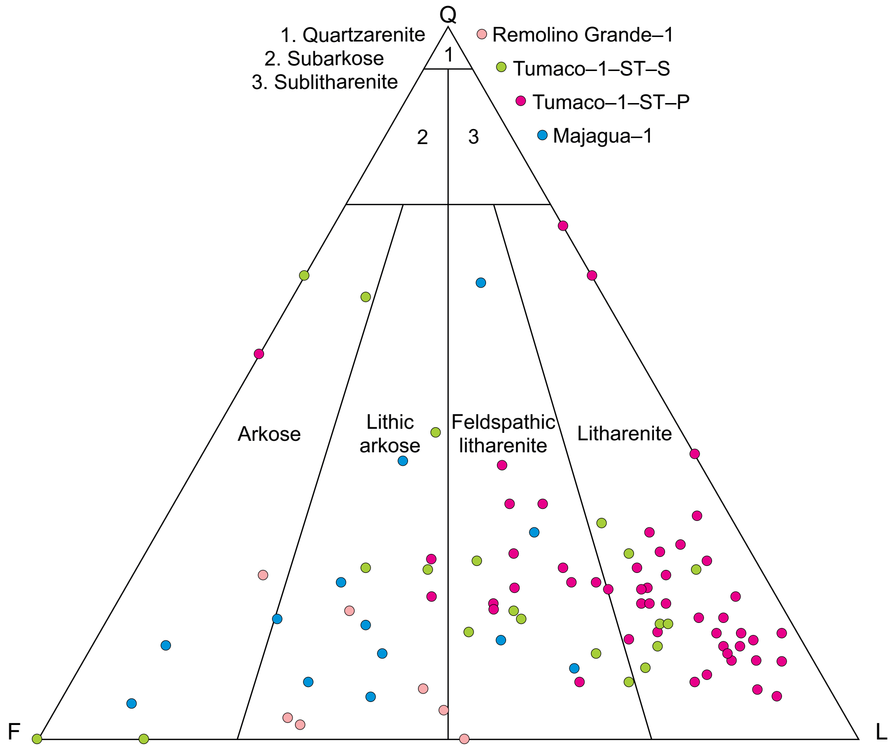

Figure 8. Classification of sandstones (Folk, 1974) in cores from the Tumaco 1–ST–S and Tumaco 1–ST–P wells, and sandstone fragments of the ditch cuttings from the Majagua–1, Remolino Grande–1, and Tumaco 1–ST–P wells. Based on Cortés et al. (2019), and Agencia Nacional de Hidrocarburos & Universidad de Caldas (2011a, 2011b).

4.4.1. Seismic Lines

The middle Miocene reflectors onlap onto the lower Miocene deposits towards the E of the basin (Figure 3a). They became thinner in the Remolino Grande–Gorgona Structural High to the west. In the Tumaco offshore basin, the middle Miocene reflectors are in toplap against Pliocene reflectors (Figure 3a). In the strike seismic line, they are conformable with the lower and upper Miocene reflectors (Figure 3b). It is not clear that the middle Miocene reflectors were affected by the mud diapir; therefore, they are marked with a dotted line.

4.4.2. Lithology

In the Remolino Grande–1 well, the middle Miocene deposits consist of amalgamated sandstones interbedded with conglomerates; in lower proportions, sandy siltstones and calcareous sandstones are present. In the Majagua–1 well, they mainly consist of sandstones and conglomerates interbedded with mudrocks (Figure 4), with abundant foraminifera and mollusk shells. These rocks are interpreted as delta front deposits probably related to a relative shallowing of the depositional environment (Agencia Nacional de Hidrocarburos & Universidad de Caldas, 2011a). In the Tumaco 1–ST–P well, middle Miocene rocks are composed of mudrocks, sublitharenites, feldspathic litharenites, litharenites, and conglomerates. Fossils of scaphopods, pelecypods, ambulacres, gastropods, and echinoderms are present in this interval. This succession is interpreted as accumulated in different environments of a deltaic system (prodelta, estuarine bars, river mouth bars, and lagoons; Agencia Nacional de Hidrocarburos & Antek, 2013).

4.4.3. Biostratigraphy

The Remolino Grande–1 well contains useful biostratigraphic events such as the last occurrences of *Globorotalia peripheroronda, H. ampliaperta*, and *S. heteromorphus*, which were found together with sporadic abundances of *Fohsella fohsi, Globigerinoides sicanus*, and *Orbulina universa*. Microfossils of this well do not support an age younger than the nanoplankton biozone NN6 (late Serravallian at 1990', Figure 5). Nevertheless, this information linked to the 11.5 Ma maximum depositional age of detrital zircon at ca. 1450' allows the location of the middle – upper Miocene limit between ca. 1450–1990' (Figures 4, 5). Biostratigraphic records of Tumaco 1–ST–P and Majagua–1 wells have discontinuous abundance patterns of microfossils and very abundant reworked assemblages (Figure 5). In the case of the Tumaco 1–ST–P well, reworked species of *Cyclicargolithus floridanus* and *S. heteromorphus* were reported within younger microfossils of *Discoaster kugleri*. Figure 5

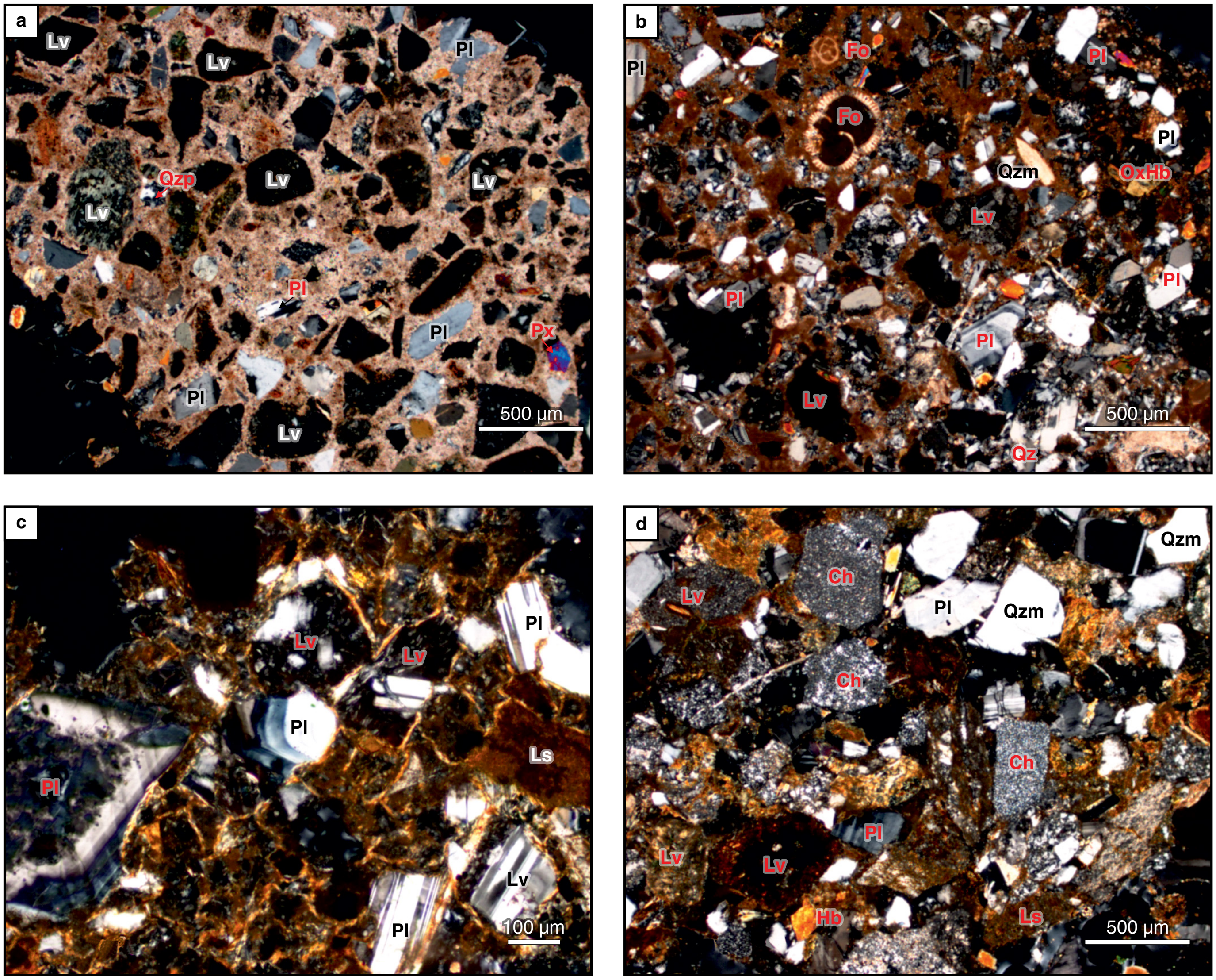

Figure 9. Microphotographs of the Majagua–1 well. **(a)** Sample MIPP–01: Feldspathic litharenite with plagioclase, volcanic lithic, pyroxene, and calcareous cement. Crossed nicols. **(b)** MIPP–13: Feldspathic litharenite with volcanic fragments, plagioclase (zoned and twined), quartz, oxyhornblende, and foraminifera. Crossed nicols. **(c)** MIPP–18: Feldspathic litharenite with plagioclase, volcanic and sedimentary lithics. Crossed nicols. **(d)** MIPP–28: Feldspathic litharenites with volcanic fragments, plagioclase, quartz, chert, and calcareous cement. Crossed nicols. Abbreviations: (Lv) volcanic lithic; (Ls) sedimentary lithic; (Ch) chert; (Pl) plagioclase; (Qz) quartz; (Qzp) polycrystalline quartz; (Qzm) monocrystalline quartz; (Hb) hornblende; (OxHb) oxyhornblende; (Px) pyroxene; (Fo) foraminifera.

shows the stratigraphic equivalence of the Remolino Grande–1, Majagua–1, and Tumaco 1–ST–P wells, with the calcareous nannofossils and planktonic foraminifera standard biozones. This range covers the interval between zones NN4 to NN6 and N8 to N12, respectively.

4.4.4. Petrography

Ditch cutting samples from the Majagua–1 and Remolino Grande–1 wells are composed mainly by siltstones, sandy siltstones, sandstones, volcanic rocks, chert, and plagioclase (Figures 7, 8), with lower proportions of quartz grains (mono– and polycrystalline), plutonic rocks, potassium feldspar, limestones, amphibole, biotite, chlorite, pyroxene, glauconite, opaque, and bioclasts (foraminifera). The sandstone grains of the Majagua–1 and Remolino Grande–1 wells are classified as lithic arkoses, arkoses, and lower proportions of feldspathic litharenites (Figures 7, 8) and are composed of fine to coarse, angular to rounded grains, with a high content of plagioclase (23–68 %), rock fragments (8–47 %), and a minor proportion of quartz (2–23 %). The lithic fragments are mainly volcanic of intermediate composition (8–39 %), sandstones (2–3 %), shales (1%), chert (3–8 %), and graphite schists (1–2 %) (Figure 7). Accessory minerals as oxyhornblende and hornblende (1–5 %), epidote (1–3 %), muscovite (< 1%), biotite (1–3 %), and chlorite (1–2 %) are present. In the Tumaco 1–ST–P

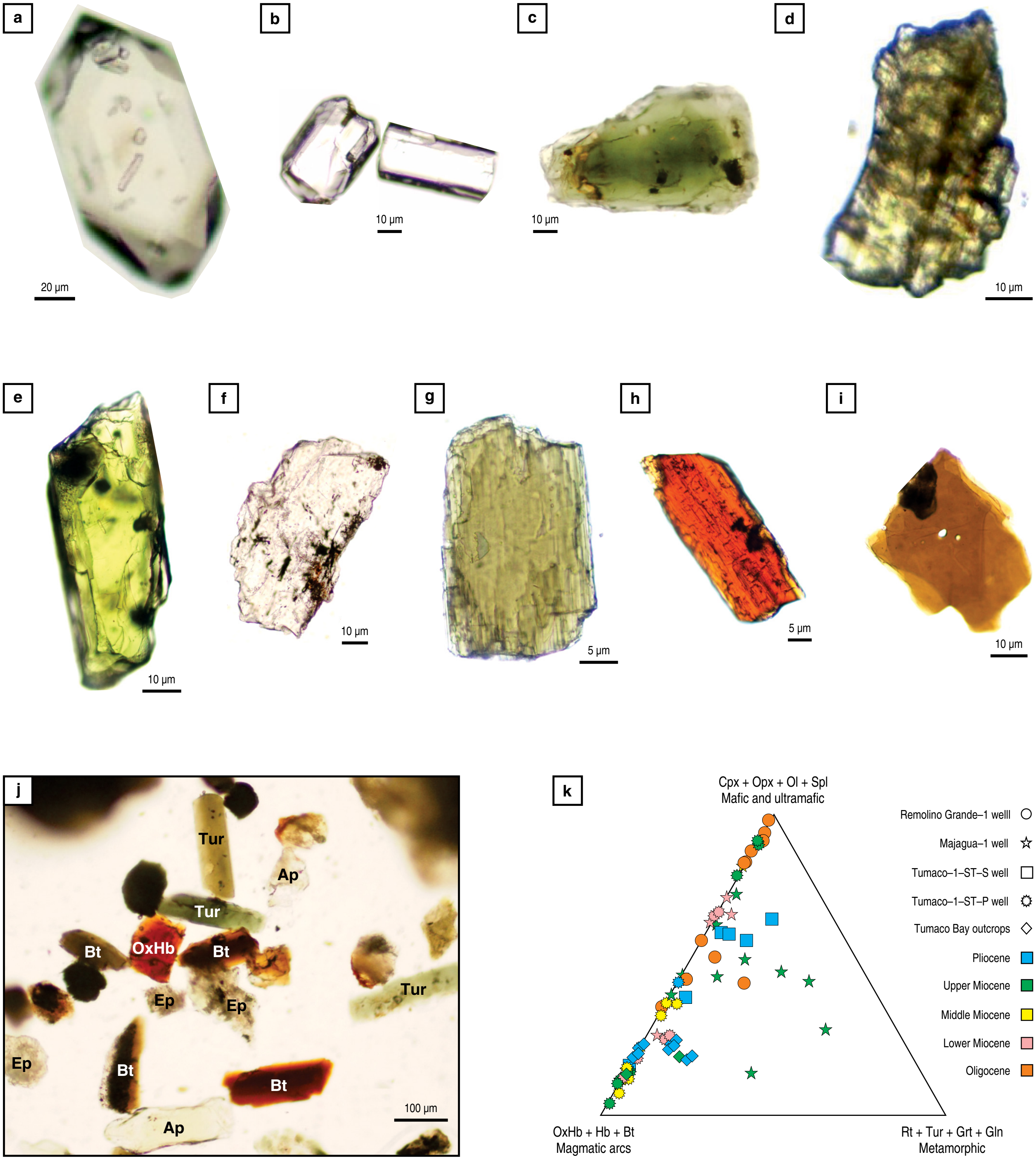

Figure 10. Some heavy minerals found in the sandstones of the Tumaco Basin. **(a)** Zircon. **(b)** Apatite. **(c)** Green tourmaline. **(d)** Epidote. **(e)** Augite. **(f)** Hypersthene. **(g)** Hornblende. **(h)** Oxyhornblende. **(i)** Biotite. **(j)** Association of ultrastable and unstable phases: (Tur) Tourmaline + (Ap) Apatite + (Bt) Biotite + (Ep) epidote + (OxHb) Oxyhornblende. **(k)** Triangular diagram with groups of heavy minerals and their source rocks.

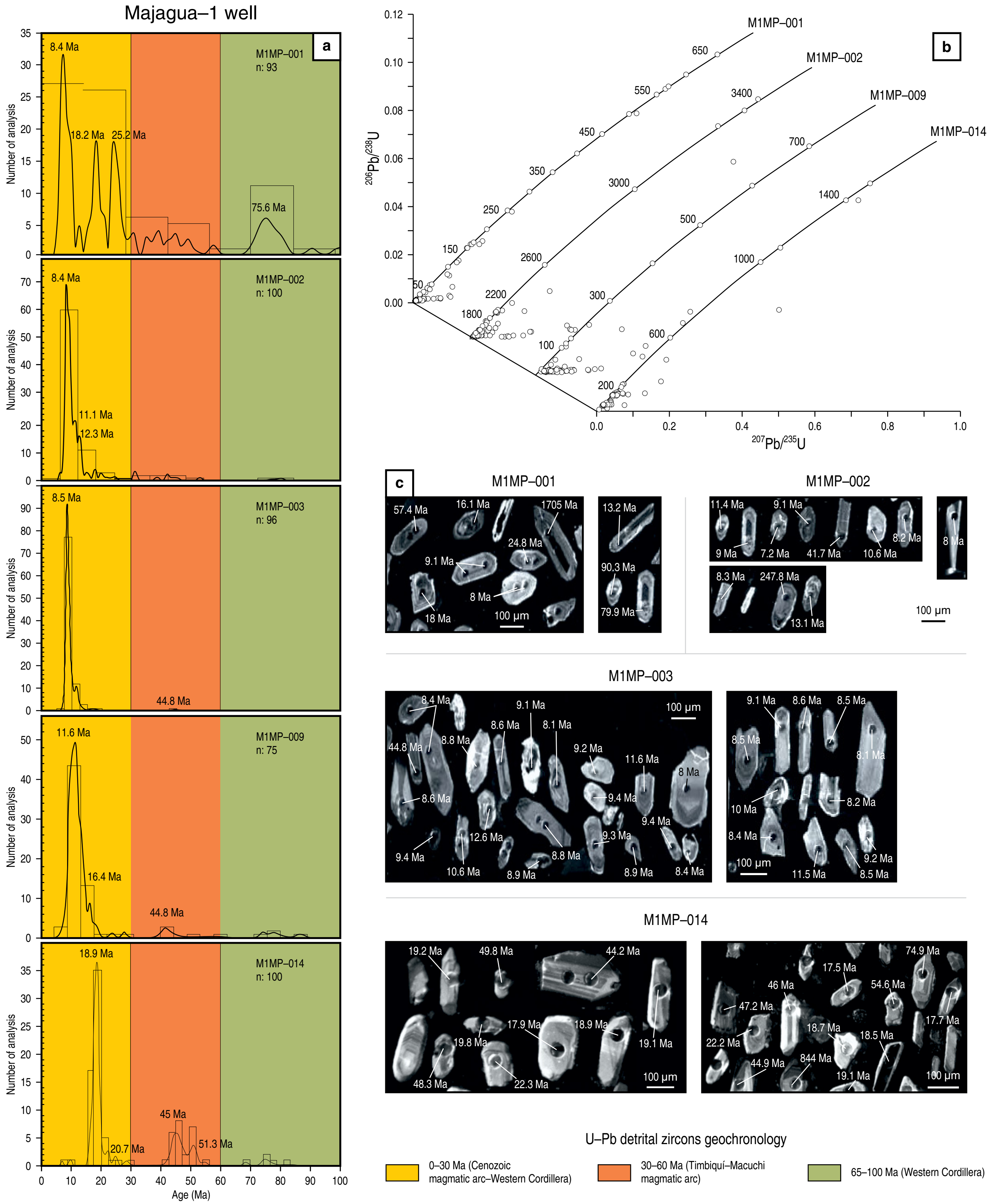

Figure 11. (a) Relative probability diagrams of U/Pb ages of detrital zircons from the Majagua–1 well. **(b)** Concordia diagrams of the samples (Tera–Wasserburg diagrams, Ludwing, 2003). **(c)** Cathodoluminiscence of some zircon crystals. The presence of zircons with volcanic morphology (euhedral grains with length/width ratios >3) and U/Pb ages between 12 and 8 Ma is noteworthy (from Echeverri et al., 2015b).

well, sandstones are mainly litharenites and lithic greywackes. Rock fragments are mainly sedimentary, metamorphic, volcanic and plutonic mafic and felsic (Agencia Nacional de Hidrocarburos & Antek, 2013).

4.4.5. Heavy Minerals

Two samples from the Remolino Grande–1 well and three from the Majagua–1 well were analyzed (Figures 6, 7). In the Remolino Grande–1, stable phases are almost absent, with only 1% zircon. The unstable phases include apatite (13–23 %), clinopyroxene (12 %), orthopyroxene (1–2 %), hornblende (2–9 %), and minerals of the epidote group (59–61 %). Oxyhornblende, biotite, chlorite, and olivine are present in low proportions (≤ 2%). In the Majagua–1 well, a higher proportion of unstable with respect to the ultrastable phases was found (Figure 7). The ultrastable phases include zircon (7–21 %) and traces of tourmaline (< 1%). The unstable phases include apatite (29–75 %), minerals of the epidote group (6–29 %), biotite (2–5 %), clinopyroxene (1–25 %), chlorite (1–3 %), hornblende (≤ 1%), actinolite (≤ 1%), and traces of oxyhornblende and ortopyroxene. The unstable phases such as apatite, pyroxene, and epidote are dominating and increase with respect to the Oligocene beds in the Tumaco 1–ST–P well (Agencia Nacional de Hidrocarburos & Antek, 2013). In the Tumaco 1–ST–P well, a greater proportion of unstable phases compared to stable was also observed. The ultrastable phases include zircon (1%) and traces of tourmaline (< 1%). The unstable phases include hornblende (48–68 %), minerals of the epidote group (6–26 %), apatite (< 1–4 %), clinopyroxene (2–28 %), ortopyroxene (< 1–18 %), chlorite (1–3 %), and garnet (< 1–2 %).

4.4.6. Detrital Geochronology

Two samples from the Remolino Grande–1 well were analyzed (RG–MP–007: depth 2640–2760'; RG–MP–006: depth 2140–2380'). These samples have maximum depositional ages of 13.3 Ma and 13.1 Ma (Serravallian), respectively. They show similar patterns of zircon distributions: the most abundant population is 12–14 Ma, followed by 22–24 Ma and 45 Ma. Very low percentages of Late Cretaceous, Triassic, early Paleozoic, and Precambrian zircons were recognized (Figure 12).

4.5. Upper Miocene – Pliocene

This time interval has been partially identified in the Remolino Grande–1 (0–1990'), Majagua–1 (0?–10500'), Tumaco 1–ST–P (32–7000'), Tumaco 1–ST–S (0?–1899.6'), and Tumaco Bay outcrops.

4.5.1. Seismic Lines

To the east of the basin, the upper Miocene reflectors onlap over the lower – middle Miocene and the basement rocks (Figure 3a). Towards the west of the basin, some reflectors come to the surface in the Remolino Grande–Gorgona Structural High, forming gentle hills, which are currently subject to erosion. In the offshore basin, the upper Miocene reflectors toplap against the Pliocene (Figure 3a). On the strike line, both the upper Miocene and the Pliocene reflectors become thinner towards the south of the studied area (Figure 3b).

Pliocene reflectors can be divided into three sets. (i) The lower set rests on the Cretaceous basement to the east, and onlap onto the Paleogene (Figure 3a). Towards the west, it decreases in thickness, and is truncated by the reflectors of the middle set. (ii) The middle set shows a clear progradation of the eastern and western reflectors towards the depocenter of the basin showing downlap over the set 1 (red arrows in Figure 3a) and a decrease in their thickness in the same direction. (iii) The upper set truncates the reflectors of the middle set and pinches out towards the E and W borders of the basin (Figure 3a). In the Tumaco offshore basin, Pliocene beds are covering the middle and upper deposits, forming an erosional truncation (toplap) (Figure 3a). In the Remolino Grande–1 well, there is no Pliocene record, probably related to erosion or no deposition during the Remolino Grande–Gorgona Structural High uplift.

4.5.2. Lithology

In the Remolino Grande–1 well, upper Miocene beds are composed by thick beds of sandstones and sandy siltstones interlayed with thin beds of mudrocks. Above 760', mudrocks with thin sandstone beds are dominant (Figure 4). In the Majagua–1 well, the lower part of the beds is composed of sandstones interbedded with sandy mudstones, mudrocks and, in lower proportions, conglomerates. In the upper part (above ca. 8000'), there is a sudden increase in thick sandstone beds (Chagüí Formation; Figures 2, 4). The sandstones in some cases can be calcareous. Remnants of mollusks and carbonized organic matter are locally abundant. The thickness and frequency of sandstones vs. fine grained sedimentites change through the time; for this reason, several units have been proposed (e.g., Angostura, Chagüí, and San Agustín Formations; Agencia Nacional de Hidrocarburos & Universidad de Caldas, 2011a; Suárez, 1990). These deposits can be associated with deltaic systems. Good exposures of these rocks can be studied in the coastal cliffs of the Tumaco Bay (Figure 13). Normal faults, slumped beds, and clastic dykes are common in these units (Figure 13). In the Tumaco 1–ST–P well, mudrocks, calcareous mudrocks, laminated sandstones, and matrix–supported conglomerates can be observed; they are generally bioturbated. An increase upward in volcanic materi-

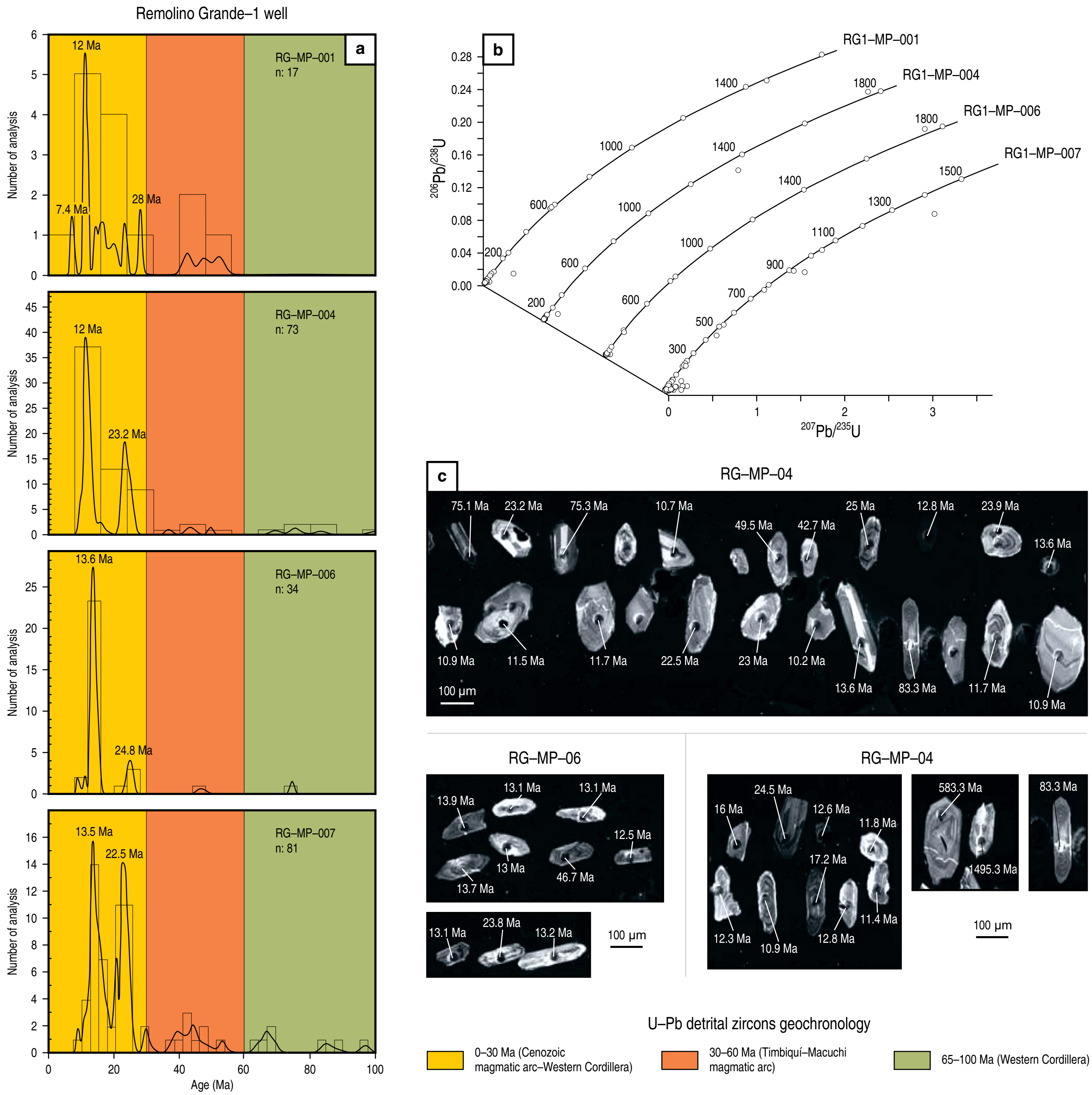

Figure 12. (a) Relative probability diagrams of U/Pb ages of detrital zircons from the Remolino Grande–1 well. **(b)** Concordia diagrams of the samples. **(c)** Cathodoluminiscence of some zircon crystals (from Echeverri et al., 2015b).

als is notorious. They were interpreted as fluvial and deltaic deposits (Agencia Nacional de Hidrocarburos & Antek, 2013).

During the latest Miocene – Pliocene (Messinian – Zanclean), in the southern part of Tumaco Basin, more than 1300' (400 m) of thick lenticular layers of sandstones and conglomerates, with an important volcanic input (Cascajal Formation of Echeverri et al., 2016), were accumulated and interlayered with some mudrocks and muddy sandstone beds. Locally, bivalves, gastropods, foraminifera, echinoderms, crustaceans, and well–preserved plant remains were found. The unit was accumulated in a deltaic system influenced by volcanism (Echeverri et al., 2016).

4.5.3. Biostratigraphy

Tumaco 1–ST–P and Majagua–1 are the only wells from which middle Miocene microfossils were recovered. However, our in-

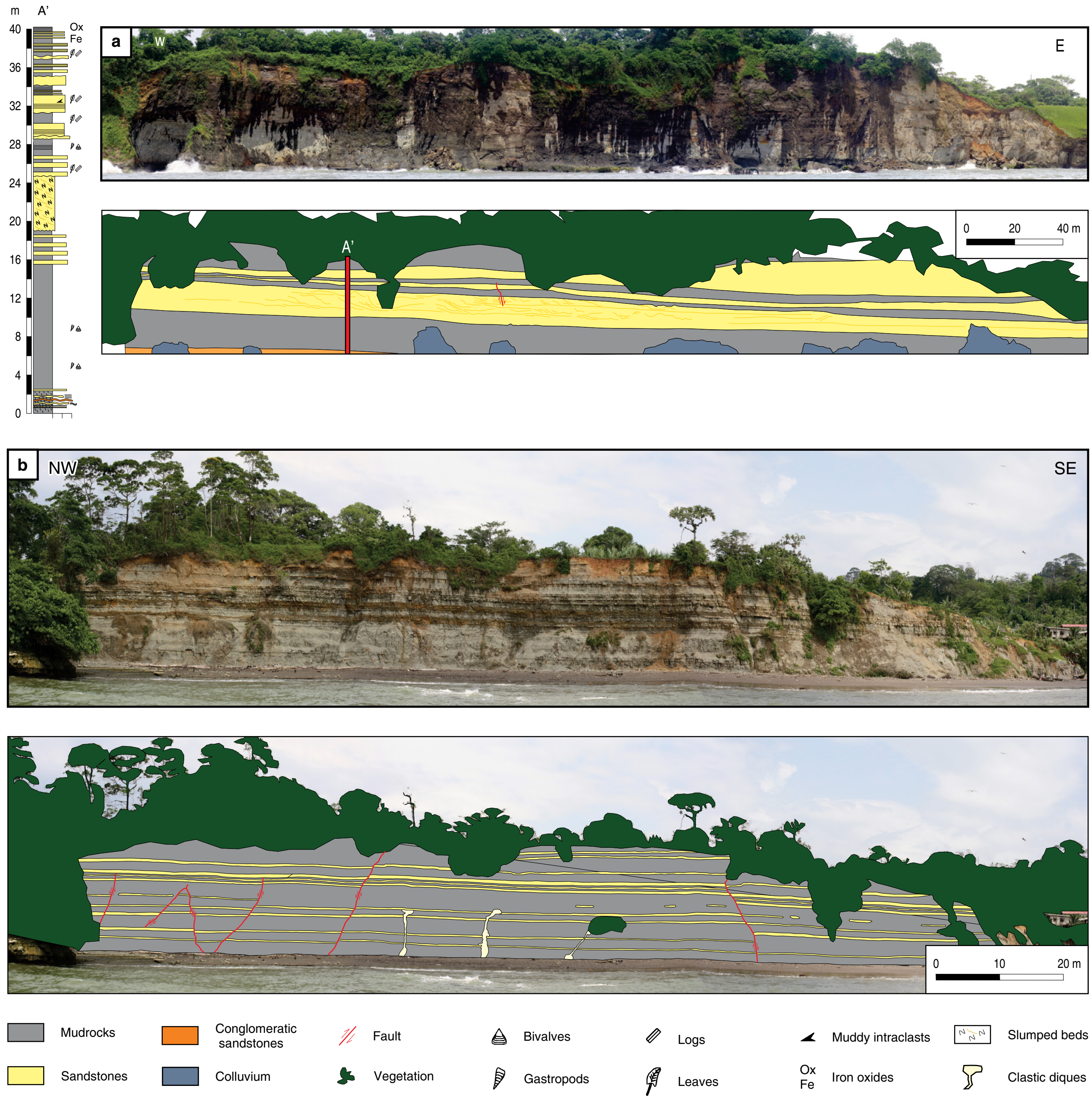

Figure 13. Panoramic pictures of Tumaco Basin outcrops (San Agustín Formation, Tortonian – Messinian). **(a)** Curay. **(b)** La Chorrera. The facies are mainly mudrocks interbedded with sandstone beds. Notice the presence of slumped beds and clastic dykes (see Figure 1 for location).

terpretation suggests that these wells record Tortonian sedimentation. This is supported by the occurrence of *Catinaster coalitus, Discoaster bellus*, and *D. hamatus* in both sites. Detailed studies conducted on the Tumaco 1–ST–P well have demonstrated that this assemblage is very abundant and highly resistant to dissolution, making them useful in biostratigraphy. The Serravallian/Tortonian (middle/upper Miocene) boundary was placed at 7000' in the Tumaco 1–ST–P well according to the last occurrence of *E. kugleri* (Figure 5). After this, we observed several bioevents of the calcareous nannofossils *C. coalitus, D. hamatus,* and planktonic foraminifera *Neogloboquadrina acostaensis* and *Paragloborotalia mayeri*, as well as sporadic nannofossils *D. bellus, D. bollii, D. brouweri*, and *S. abies*. An increase of the accumulation rate is inferred during the Tortonian at Tumaco 1–ST–P well, as these taxa are characterized by a short life span and they were found successively in the well. Alternatively, the last consistent biostratigraphic marker in the Majagua–1 well was the last occurrence of *C. coalitus* at 8820'.

As shown in Figure 5, in the Majagua–1 and Tumaco 1–ST–P wells, the equivalence with the calcareous nannofossils and planktonic foraminifera standard zones represents an interval from NN7 to NN10 and N14 to N16, respectively.

Diagnostic species such as *D. neohamatus, D. berggrenii, D. quinqueramus, D. asymmetricus*, and *Globorotalia tumida* were identified in the upper part of the Tumaco 1–ST–P and Majagua–1 wells, occasionally associated with abundant reworked microfossils (mainly Cretaceous and Paleogene). Although it is difficult to identify a succession of standard zonations, the microfossil assemblages allow the designation of a Messinian – Piacenzian age. Palynological data in the Tumaco 1–ST–P well show the first occurrence of *Cyatheacidites annulatus* at 3950' (ditch cutting sample) (Figure 5), considered a late Miocene biostratigraphic marker in the Llanos Basin (first occurrence datum at 7.1 Ma) (Jaramillo et al., 2011).

4.5.4. Petrography

Upper Miocene ditch cutting samples from the Majagua–1 and Remolino Grande–1 wells (upper Viche and Angostura Formations) are mainly composed of mudrocks, volcanic rocks, and plagioclase. Chert, quartz (mono and polycrystalline), potassium feldspar, amphibole, biotite, pyroxene, chlorite, glauconite, and bioclasts (foraminifera, algae, bivalves) are present in a lower proportion. In the middle part (Chagüí Formation), the samples have mainly volcanic fragments and plagioclase, as well as sedimentary rocks (shales, sandstones, and cherts) (Figure 7). In some levels, pyroxene, amphibole, and biotite are frequent. In addition, plutonic grains, potassium feldspar, quartz (mono and polycrystalline), tourmaline, apatite, calcite, chlorite, epidote, glauconite, and foraminifera are present in lower proportions. In the top of the Majagua–1 well, the samples mainly have volcanic grains, plagioclase, and sedimentary rock fragments (chert, shale, limestone, and bioclasts). In lower proportions, schists, intermediate plutonics, potassic feldspars, quartz (mono– and polycrystalline), pyroxenes, amphibole, tourmaline, chlorite, epidote, glauconite, and bioclasts (foraminifera) were identified.

Sandstone grains of the Majagua–1 well are classified as lithic arkoses and feldspathic litharenites (Figure 8). They are fine–grained, poorly sorted, and with angular to rounded grains (Figures 7, 8), composed mainly by plagioclase (12–54 %), quartz (1–25 %), and intermediate volcanic rock fragments (4–54 %). Sedimentary lithics are composed by sandstones (1–8 %), mudrocks (1–14 %), and cherts (1–5 %) (Figure 7). Among accessory minerals were identified oxyhornblende and hornblende (1–16 %), pyroxene (1–5 %), glauconite (1–2 %), biotite (1–6 %), chlorite (1–4 %), and epidote (1–6 %). In the Tumaco 1–ST–P well, sandstones are litharenites, feldspathic litharenites, and lower proportions of lithic arkose. Constituents are mostly volcanic. Lithics are mainly mudrocks, andesites, and diorites (Agencia Nacional de Hidrocarburos & Antek, 2013).

4.5.5. Heavy Minerals

Five samples from the Remolino Grande–1 well and ten from the Majagua–1 well were analyzed (Figures 6, 7). In the Remolino Grande–1, stable phases are scarce with tourmaline (2–10 %) and zircon (1%). The unstable phases are dominant and include apatite (3–20 %), clinopyroxene (9–33 %), orthopyroxene (1–4 %), hornblende (1–9 %), oxyhornblende (1–3 %), biotite (1–10 %), and minerals of the epidote group (31–81 %). Chlorite, olivine, and actinolite are present in low proportions (≤ 1%). In the Majagua–1 well, a higher proportion of unstable with respect to the ultrastable phases was found (Figure 7). The ultrastable phases include zircon (1–23 %) and tourmaline (1–33 %). The unstable phases include apatite (4–69 %), minerals of the epidote group (4–38 %), biotite (2–6 %), muscovite (1 %), clinopyroxene (2–19 %), ortopyroxene (< 1–5 %), olivine (1%), chlorite (1–3 %), oxyhornblende (< 1–7 %), and hornblende (1–19 %). In the Tumaco 1–ST–P well, a greater proportion of unstable phases compared to stable phases was also observed (Agencia Nacional de Hidrocarburos & Antek, 2013). The ultrastable phases only include zircon (1%), while unstable phases are dominant and include hornblende (9–72 %), minerals of the epidote group (< 1–19 %), apatite (< 1–3 %), clinopyroxene (4–3 6%), ortopyroxene (4–63 %), biotite (1–3 %), chlorite (≤ 1%), and garnet (1%).

4.5.6. Detrital Geochronology

Two samples for the Remolino Grande–1 well (RG–MP–004; depth 1210–1450' and RG–MP–001; depth 84–300') were analyzed. They have 10.4 Ma and 11.5 Ma of maximum depositional ages, respectively. These data allow the lower – middle Miocene boundary to be constrained between ca. 1450–1990' depth based on geochronologic and biostratigraphic data (Figure 5). They show similar patterns of zircon distributions: The most abundant population is 12–14 Ma, followed by 22–24 Ma and 45 Ma. Very low percentages of Late Cretaceous, Triassic, early Paleozoic, and Precambrian zircons were recognized (Figure 12).

In the Majagua–1 well, four samples (M1MP–009, depth 9100–9320'; M1MP–003, depth 3430–3950'; M1MP–002, depth 2830–3210'; and M1MP–001, depth 110–800') were analyzed. They have 9.3 Ma, 7.6 Ma, 7.5 Ma, and 6.6 Ma maximum depositional ages, respectively. Three main populations of zircons are recognized: 7–12 Ma, 16–25 Ma (especially to the top of the well), and 45–50 Ma (Figure 11). In lower proportions are late Oligocene – Miocene, Paleocene, and Late Cretaceous and Jurassic zircons, which are not abundant enough to constitute a population.

Two samples from the Tumaco 1–ST–S well, two from outcrops of the Tumaco Bay, three in the Pleistocene fans and one in recent sedimentites were also analyzed. In the Pliocene beds, similar populations of detrital zircons ages are observed: the most abundant is 4.1–7.6 Ma, followed by 6.5–7.6 Ma, 9.0–13.0 Ma, and 19.0–23.0 Ma. Very low percentages of Late Cretaceous, Triassic, early Paleozoic, and Precambrian zircons were recognized. The maximum depositional ages in two samples of the Tumaco 1–ST–S well were 6.5 Ma (1257') and 4.1 Ma (400') (Figure 5).

4.6. Pliocene – Holocene

Pliocene – Holocene volcaniclastic fans were identified in the eastern border of the basin (Figure 14). The volcanic source probably came from an old Cumbal Volcano and from the Azufral volcanic activity in the Western Cordillera. Three alluvial fans can be differentiated, which prograde in the basin through time (Figure 14): (i) The oldest fan (Pliocene?), 1560 km^2, is strongly dissected and controlled by the Junín Sambianí Fault, and it is formed by lahar and debris flow deposits mainly composed of dacitic and andesitic rock fragments. (ii) A younger fan, 160 km^2, formed by lahar and debris flow deposits, is mainly composed of andesitic rock fragments. (iii) The youngest fan covers 2030 km^2. It is formed by lahar, debris flow, and stream flow deposits and is mainly composed of dacitic pumice fragments. This deposit partially overlays the Cascajal Formation in unconformity, and they are interlayered with recent littoral sediments along the Pacific coast.

The youngest volcanoclastic fan has 2.04 Ma as its maximum depositional age (Figure 14). In the Pleistocene fans and the recent sediments, detrital zircon populations of 26–20 Ma, 14–11 Ma, 9–6 Ma, and 4–3 Ma were identified. These detrital populations are in concordance with those present in the underlying stratigraphic sequence. However, there is a significant presence of zircons between 3–1.5 Ma, which records the most recent activity of the magmatic arc (Figure 14). In the Tumaco Bay outcrops, five samples were analyzed in the Pliocene – Pleistocene deposits (Figure 1). In general, stable phases occur in minor proportions compared with unstable ones. The stable phases are constituted by zircon (10–21 %), tourmaline (5–9 %), and rutile (2%). The unstable phases are dominant and include apatite (3–7 %), pyroxene (10–16 %), hornblende (24–33 %), biotite (24–29 %), and olivine (3–5 %). Chlorite and minerals of the epidote group are present in very low proportions (≤ 1%).

Holocene deposits are mainly composed by coastal and fluvial sediments from the Patía and Mira Rivers. To the upper part of the Tumaco 1–ST–S well, an unconsolidated sedimentary sequence of (ca. 32'; 9.8 m) sands and muds was identified. There were two ^{14}C AMS ages in organic sediments, 4360 ± 30 BP and 4150 ± 30 BP (Holocene). These sediments belong to the deltaic plain of the Mira River (López et al., 2012).

5. Interpretation

5.1. Cretaceous – Paleogene

The Upper Cretaceous volcano–sedimentary succession of Remolino Grande probably originated in an oceanic arc during the Late Cretaceous (Echeverri et al., 2015a). This unit and its basement collided obliquely against the western margin of Ecuador and Colombia during the Late Cretaceous – Paleogene, which generated thrusting, folding, and clastic sedimentation (Barrero et al., 2006; Moreno–Sánchez & Pardo–Trujillo, 2003; Pindell & Kennan, 2009; Villagómez et al., 2011). The sedimentary record of the Remolino Grande–1 well shows a Upper Cretaceous (Maastrichtian) – Eocene (ca. 20 Ma) unconformity, which could be associated with this tectonic event. In northern Ecuador, the accretion of the Piñon–Naranjal Terrane occurred at ca. 58 Ma (Paleocene) (Jaillard et al., 2009). The presence of Eocene plutonic and volcanic rocks in the Western Cordillera (Agencia Nacional de Hidrocarburos & Geología Regional y Prospección, 2011; Barbosa–Espitia et al., 2016) suggests that an Eocene volcanic arc was developed after the collision of the Tumaco Basin basement with the continental margin (Arco de Ricaute of Spadea & Espinosa, 1996). Over these rocks, upper Eocene – lower Miocene fine–grained clastic sedimentary successions were discordantly accumulated in shelf and prodelta environments (Lutitas de Remolino Grande Formation or 1 Sur Unit; Figure 2).

5.2. Early – Middle Miocene

The facies recorded in the wells suggest sedimentation in shelf, prodelta, and deltaic environments (Angostura, Viche, and Cayapas Formations; Figure 2; Agencia Nacional de Hidrocarburos & Universidad de Caldas, 2011a; Agencia Nacional de Hidrocarburos & Antek, 2013). The common presence of muddy matrix and the angularity and poor sorting of grains in sandstones and conglomerates suggest first–cycle sedimentation and rapid burial. During the early Miocene, an ca. 5 Ma unconformity was identified in the Remolino Grande–1 well (Figure 5). This unconformity could be related to an exhumation pulse of the Western Cordillera and the Remolino Grande–Gorgona Structural High, linked to an increase in the orthogonal convergence rates of the Nazca–South American Plates (cf. Pardo–Casas & Molnar, 1987; Somoza & Ghidella, 2012). Based on thermochronologic analyses of the Gorgona Island, the Tumaco Basin, and the southern part of the Western Cordillera, Barbosa–Espitia et al. (2013a) interpreted a progressive and generalized exhuma-

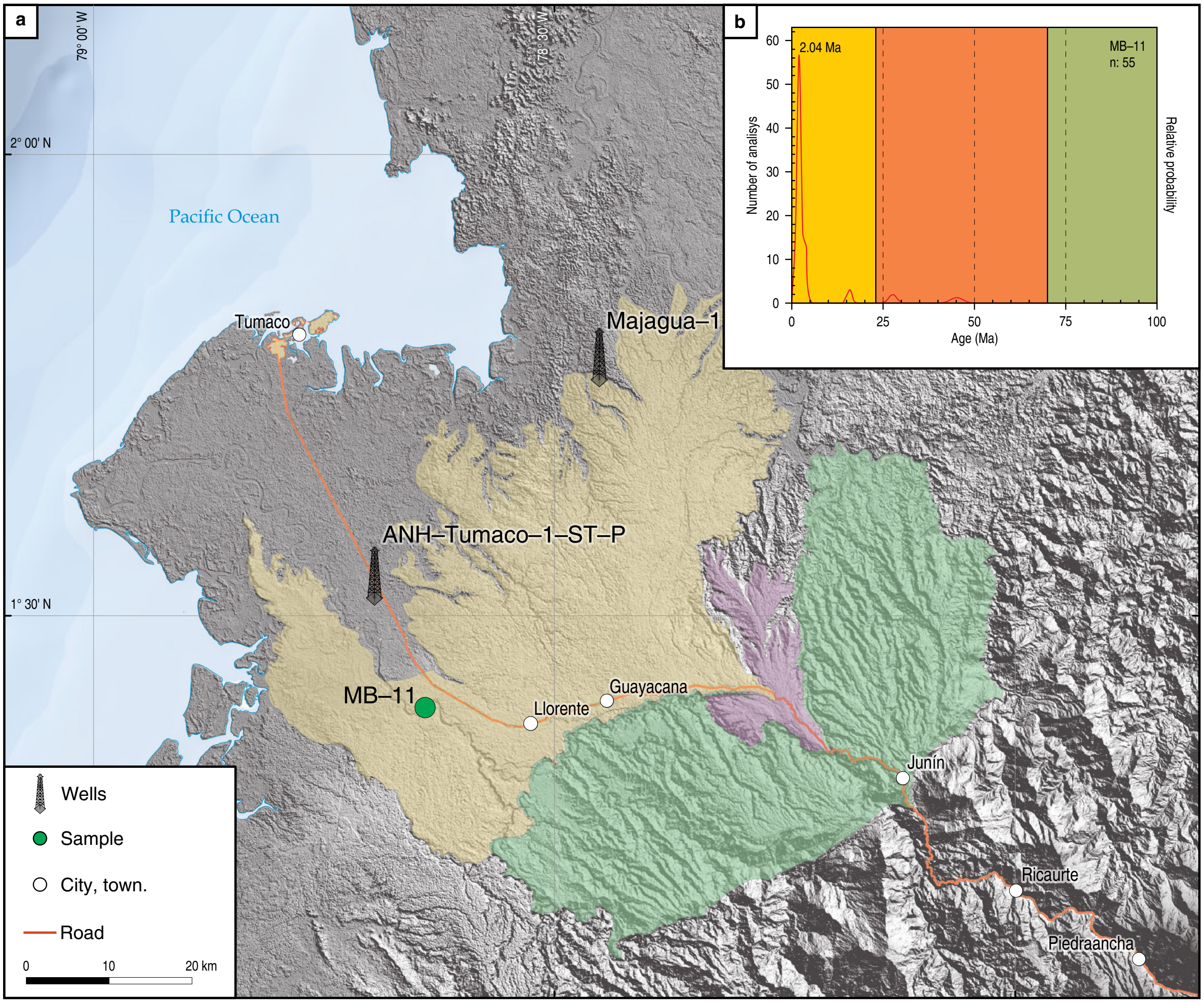

Figure 14. (a) Distribution of Pliocene – Pleistocene volcanoclastic fans in the southern Tumaco Basin. In green: the oldest fan; purple: the younger fan; brown: the youngest fan (see explanation in the text). **(b)** Relative probability diagrams of U/Pb ages of detrital zircons from the MB–11 sample (color conventions as in Figure 11).

tion cooling in the area between 24–22 and 20–16 Ma. Thermochronologic analyses of the Western and Eastern Cordilleras of Ecuador also recorded an exhumation event between 25–22 Ma, which suggests a regional event linked to plate–scale kinematic changes (Spikings & Crowhurst, 2004; Spikings et al., 2005). In Ecuador, a middle Miocene cooling event has been attributed to the increase in compressive stress during the collision of the Carnegie Ridge with the South American margin, which started at ca. 15 Ma (Spikings et al., 2010). According to López–Ramos (2009) the division of the Tumaco Borbón and Manglares (Tumaco offshore) Basins occurred in the middle Miocene time and was related to the subduction of the young and hot Nazca Plate and the decrease in the convergence rate.

Three compositional associations in lower – middle Miocene sandstones are indicative of sediment sources: (i) Abundance of plagioclase and intermediate volcanic fragments can be associated with volcanic igneous rock sources. (ii) Olivine and pyroxenes (mainly augite) are related to mafic–ultramafic igneous rocks (Figure 10). (iii) Potassium feldspar, quartz, amphibole, and occasionally biotite are related to acid and/or intermediate plutonic rocks. This can be compared to the present–day basement of the Western Cordillera, where upper Eocene and Oligocene granitoids intrude the Cretaceous oceanic sedimentary and basic igneous rocks (Figure 15; Barbosa–Espitia et al., 2016; Gómez et al., 2015). In the Majagua–1 well, there is more than 50% sedimentary lithics with respect to igneous fragments and feldspars. In contrast, the Remolino Grande–1 well shows an increasing tendency in the content of volcanic, plutonic fragments, and feldspars in the middle Miocene (Figures 6, 7). The analysis of heavy minerals in the Remolino Grande–1 well shows a domain of unstable phases (mainly epidote, augite, and hornblende), and the Majagua–1 well presents a domain of ultrastable phases (mainly zircon and apatite). These compositional contrasts are probably related to different source areas or disconnection in the paleo–drainage systems or may also be influenced by the formation of topographic highs that controlled the drainages and acted as sedimentation barriers.

The 24–18 Ma and 12–14 Ma most frequent populations of detrital zircons indicate a magmatic activity during these periods in the vicinity of the basin, which can be associated with Western Cordillera plutonic bodies that intrude the Cretaceous oceanic sedimentary and basic igneous rocks of the Western Cordillera (Agencia Nacional de Hidrocarburos & Geología Regional y Prospección, 2011; Barbosa–Espitia et al., 2016; Echeverri et al., 2015b). Magmatic activity close to the source is also consistent with the preservation of feldspars and volcanic fragments and is associated with the erosion of middle–upper crustal levels in orogenic zones with magmatic activity. The occurrence of chert and other sedimentary lithics in the sandstones, as well as Mesozoic, Paleozoic, and Precambrian detrital zircons, suggests reworking of pre–Miocene sedimentary sequences of the Western Cordillera or, alternatively, a connection with the Central Cordillera basement. This connection could explain the presence of metamorphic fragments in very low percentages. Additionally, marine fossils (mollusks and foraminifera) have been reported in the rocks of the Cauca–Patía Basin for the Oligocene – Miocene interval (León et al., 1973). This basin is located to the east of the Tumaco Basin between the Central and Western Cordilleras, which could indicate that the Tumaco and Cauca–Patía Basins were connected and that some sediments came directly from erosion of the Central Cordillera basement.

5.3. Late Miocene – Pliocene

In general, the presence of sandstones and conglomerates in the Majagua–1 and Remolino Grande–1 wells, as well as the abundance of mollusks and carbonized organic matter, suggest deposition in the delta plain and nearshore environments (San Agustín and Chagüí Formations; Figure 2). Fine–grained intervals with abundant mollusks and foraminifera could be associated with the lower delta front–prodelta transition. Agencia Nacional de Hidrocarburos & Antek (2013) proposed sedimentary environments varying from fluvial channels, estuarine and mouth bars, delta front and prodelta environments in the Tumaco 1–ST–P well. During this period, an increase in the sedimentation rate is notorious (Figures 5, 15).

The late Miocene increase in the sedimentation rate may be related to high subsidence in the basin (Echeverri, 2012; López–Ramos, 2009) and to the increase in the volcanic activity of the magmatic arc. López–Ramos (2009) suggests that the considerable sediment accumulation in the Tumaco Basin would have resulted from crustal buckling due to horizontal stress transfer into the overriding plate and the erosion of the Western Cordillera. He also indicates that the Remolino Grande Gorgona High was uplifted and allowed sediments to dam in the Tumaco onshore basin. Late Miocene – Pliocene uplift pulses (ca. 14–10 and ca. 6–4 Ma) recognized in southwestern Colombia (Barbosa–Espitia et al., 2013b) could be related to the following: (i) Subduction of the young oceanic crust with change in the subduction angle between Nazca and the South American Plate (Echeverri et al., 2015b), (ii) orthogonal convergence of the Nazca Plate (Pardo–Casas & Molnar, 1987; Somoza, 1998), or (iii) the collision of a buoyant slab segment, derived from the Nazca Plate, such as a small ridge or seamount, similar to, or being part of, the Carnegie Ridge, and (iv) the collision of the Panamá–Chocó Block (Barbosa–Espitia et al., 2013a).

López–Ramos (2009) indicated a upper Miocene (Tortonian) unconformity (called U2) based on seismic reflectors in the Tumaco Basin. It can be associated with a facies change in the Majagua–1 (8000'; base of the Chagüí Formation) and the Tumaco 1–ST–P wells (ca. 5400'; base of the Tangareal del Mira Formation of Agencia Nacional de Hidrocarburos & Antek, 2013) (Figure 5). This unconformity can be related with an eustatic sea level drop (10.5 Ma; Haq et al., 1987; López–Ramos, 2009). Based on thermochronological constraints, Barbosa–Espitia et al. (2013b) proposed that the Remolino Grande–Gorgona Structural High was uplifted between 14–10 Ma. This is also supported by the common presence of early Miocene reworked microfossils (Figure 15).

During the late Miocene, the upward increase in the proportion of unstable minerals such as plagioclase, pyroxene, oxyhornblende, hornblende, and volcanic fragments indicates an intensification of magmatic activity (Figure 7). This is in agreement with a dominant 12–8 Ma zircon population. The presence of microcline and biotite, as well as the occurrence of the 25–18 Ma and 50–30 Ma zircon populations, suggest the onset of the erosion of granitoids (Figures 6, 7), which could be associated with the Western Cordillera basement (e.g., Piedrancha Granodiotrite, Nulpi Gabronorite, and ca. 44 Ma dikes intruding the Timbiquí Formation; Figure 15; Agencia Nacional de Hidrocarburos & Geología Regional y Prospección, 2011a; Agencia Nacional de Hidrocarburos & Universidad de Caldas, 2011a; Barbosa–Espitia et al., 2016; Echeverri et al., 2015b). The presence of chert, sandstone, and shale fragments, as well as Mesozoic, Paleozoic, and Precambrian zircons, suggests reworking of the pre–Miocene sedimentary cover or partial connection with the Central Cordillera basement. The good preservation of plagioclase and volcanic lithics suggests short transport, rapid burial, and negligible diagenesis effects.

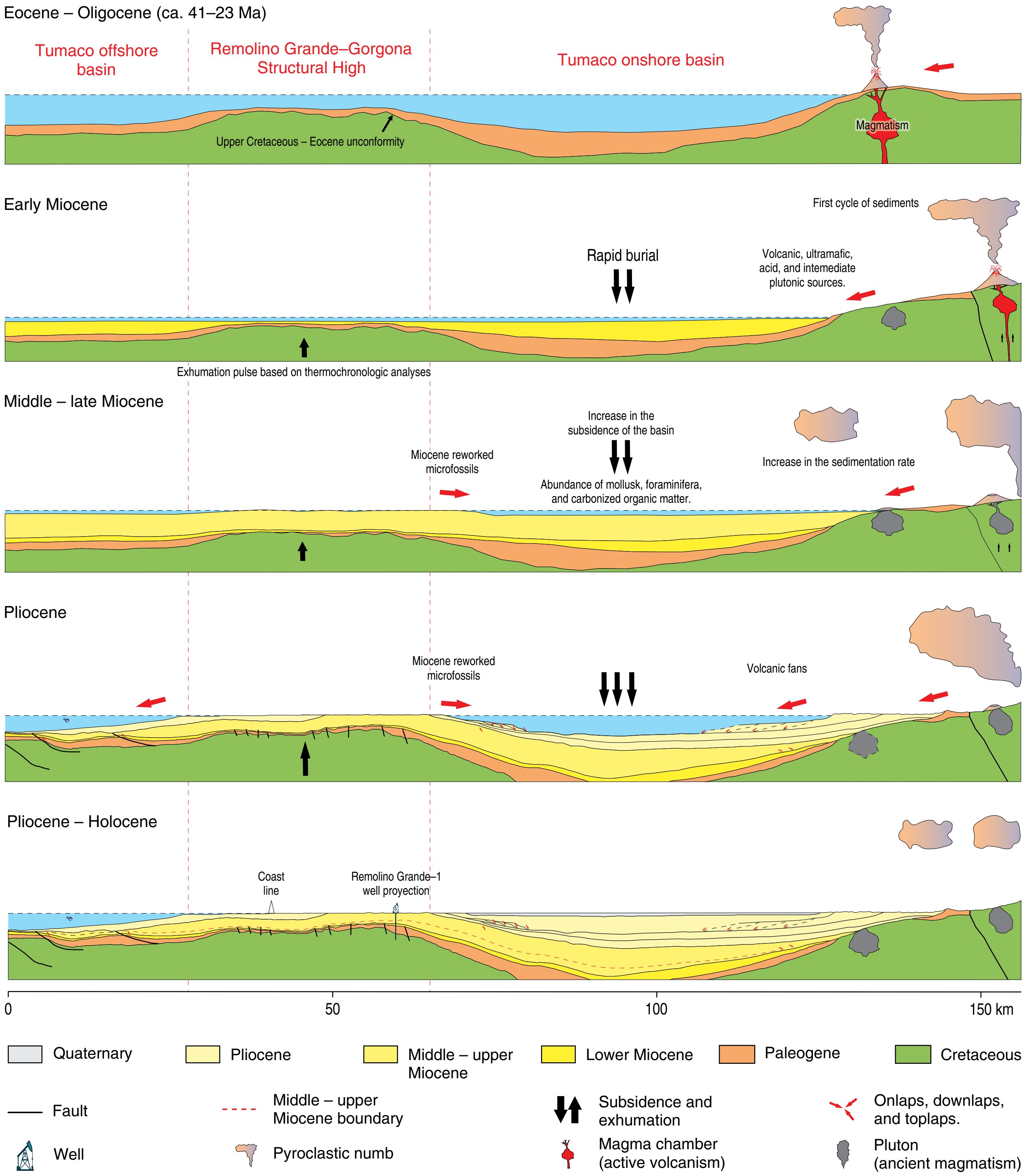

Figure 15. Eocene to Holocene geologic evolution of the southern Tumaco Basin. Not palinspatically restored. The thick red arrows indicate the direction of sediment transport. See the explanation in the text.

The Miocene – Pliocene boundary is difficult to locate with the available information. Based on paleontological data, Agencia Nacional de Hidrocarburos & Antek (2013) indicated the First Appearance Datum (FAD) of *Cyatheacidites annulatus* in the Tumaco 1–ST–P well at 3950' (ditch cutting sample). The FAD of this species is located approximately at the Tortonian – Messinian boundary (7.1 Ma, Jaramillo et al., 2011). The correlation of seismic reflectors with the Majagua–1 well (Figure 3b) allowed the establishment of a depth of ca. 6000' for this boundary. A 4.1 Ma (Zanclean) minimal age of detrital zircons from the Tumaco 1–ST–S at 400' indicates that the Miocene – Pliocene boundary is between 3950–400' (Figure 5). These difficulties show the importance of using multi–tools for chronostratigraphic interpretation, as well as the need to acquire more geological information in other places of the basin.

5.4. Pliocene – Pleistocene

During the Pliocene – Pleistocene, volcaniclastic fans were identified at the SE border of the basin (Figure 14). A progradation of seismic reflectors to the west (Figure 3a) can probably be associated with the increase in the erosion rates and/or the volcanic activity. Seismic information (e.g., onlap surfaces and eastward prograding reflectors in the western border of the onshore basin) also shows an influence of the Remolino Grande–Gorgona Structural High in the sedimentation (Figures 3a, 15).

López–Ramos (2009) identified an important Pliocene (Zanclean) unconformity (U3) marked by a deep erosional surface and an abrupt facies change (sandstones and conglomerates of the Cascajal Formation; Echeverri et al., 2016) and probably related to a regional Andean orogenic event (e.g., van der Hammen et al., 1973). Thermochronological data obtained for the Western Cordillera (Piedrancha Pluton) and in the sedimentary fill of the Tumaco Basin recorded an ca. 4 Ma exhumation event (Barbosa–Espitia et al., 2013a). This time period also coincides with a marine eustatic drop (Haq et al., 1987).

6. Conclusions

The Tumaco Basin has a through symmetric shape with ca. 26 000' (ca. 8000 m) of sediments in its depocenter. These deposits accumulated as a response to the subduction of the Farallon and Nazca Plates beneath the South American Plate, controlling subsidence, magmatic activity, and sedimentation rates.

The sedimentary fill is mainly composed of mudrocks, sandstones, and conglomerates that varied in proportion through time and accumulated in open marine to deltaic environments. The integration of biostratigraphic data obtained by the analysis of calcareous nannofossils, planktonic foraminifera, palynology, and detrital zircons allows us to produce an age model of the sedimentary deposits. The sequence starts in the Paleogene (NP19 and P16), and the upper part of the record is consistent with a Messinian – Piacenzian age. The information to establish the age of the upper Miocene – Pliocene deposits is still limited.

The Neogene sandstones of the Tumaco Basin are mainly related to nearby intermediate to mafic magmatic sources similar to the present–day Western Cordillera basement. Eocene and Cretaceous zircon populations can be related to the erosion of the Western Cordillera plutonic and volcanic rocks. The presence of Jurassic and older sources would be linked to the reworking coming from units of the Western Cordillera, although it is possible that in some areas, a direct connection with the Central Cordillera basement existed. Differences in petrography and heavy mineral associations for sediments accumulated at the same time could be related to different source areas or disconnection in the paleo–drainage systems related to topographic highs.

Detrital zircons and petrographic data indicate that sedimentation was contemporary with magmatic activity, which started at ca. 26 Ma (late Oligocene) until today, and recorded an increasing activity since the middle Miocene.

The seismic, biostratigraphic, and geochronological data enabled the identification and quantification of the duration of some unconformities in the Tumaco Basin (e.g., Late Cretaceous – Eocene, early Miocene), which seem to be related to regional and global tectonic processes, such as changes in the direction and convergence rates of tectonic plates, subduction of seamounts, and eustasy.

Acknowledgements

We thank the Agencia Nacional de Hidrocarburos and the Vicerrectoría de Investigaciones y Posgrados (Universidad de Caldas) for their financial support (contract 092 of 2009, Universidad de Caldas–Agencia Nacional de Hidrocarburos). Special thanks are due to the Instituto de Investigaciones en Estratigrafía (IIES) staff for their logistic support. People of the communities of Tumaco, Salahonda, Cascajal, and La Chorrera are greatly acknowledged for their hospitality and help during the field work. We give special thanks to many people that participate in the 092 contract: Clemencia GÓMEZ, Jairo Alonso OSORIO, Elvira C. RUÍZ, Gustavo HINCAPIÉ, Sebastián ROSERO, Marcelo JARAMILLO, Juan Carlos PATIÑO, Alejandro PINILLA, César MADRID, Rosa Ester NAVARRETE, Francisco SIERRO, Alejandra MEJÍA, Erika BEDOYA, Diana OCHOA, Silane Da SILVA, Fatima LEITE, Millerlandy ROMERO, Jenny GARCÍA, and José María JARAMILLO, among others. We also thank Jorge GÓMEZ TAPIAS (Servicio Geológico Colombiano) for his help and patience during the editing of this paper. Fundación Carolina supported AP–T with a postdoctoral stay in Salamanca (Spain) for the finalization of this document. The critical revision of the manuscript by Etienne JAILLARD and Mario SUÁREZ is greatly appreciated. We thank Daniela MATEUS ZABALA and the editorial board of the Servicio Geológico Colombiano for helpful comments that improved the chapter presentation.

References

Agencia Nacional de Hidrocarburos & Antek. 2013. Estudio integrado de los núcleos obtenidos de los pozos perforados por la ANH y de las muestras de pozo (núcleos y ripios) disponibles en la Litoteca Nacional, localizados en zonas de interés para la ANH. Pozo Tumaco–1–ST–P. Agencia Nacional de Hidrocarburos, unpublished report.

Agencia Nacional de Hidrocarburos & Geología Regional y Prospección. 2011. Cartografía geológica a escala 1:100 000 de las planchas 340, 362, 385 y 409 localizadas en la Cuenca Tumaco, así como el inherente levantamiento de columnas estratigráficas y muestreo litológico para los análisis petrográficos, bioestratigráficos, geoquímicos, petrofísicos y radiométricos. Contrato 084 de 2010, unpublished report. 207 p.

Agencia Nacional de Hidrocarburos & Universidad de Caldas. 2011a. Estudio geológico integrado en la Cuenca Tumaco onshore. Síntesis cartográfica, sísmica y análisis bioestratigráfico, petrográfico, geocronológico, termocronológico y geoquímico de testigos de perforación y muestras de superficie. Contrato 092 de 2009. Unpublished report, 191 p. Manizales, Colombia.

Agencia Nacional de Hidrocarburos & Universidad de Caldas. 2011b. Estudio integrado de los núcleos y registros obtenidos de los pozos someros (slim holes) perforados por la Agencia Nacional de Hidrocarburos. Informe Final Contrato 093 de 2009. unpublished report.

Agnini, C., Fornaciari, E., Raffi, I., Catanzariti, R., Pälike, H., Backman, J. & Rio, D. 2014. Biozonation and biochronology of Paleogene calcareous nannofossils from low and middle latitudes. Newsletters on Stratigraphy, 47(2): 131–181. https://doi.org/10.1127/0078-0421/2014/0042

Aleman, A. & Ramos, V.A. 2000. Northern Andes. In: Cordani, U.G., Milani, E.J., Thomaz–Filho, A. & Campos, D.A. (editors), Tectonic evolution of South America. 31st International Geological Congress. Proceedings, p. 453–480. Rio de Janeiro, Brazil.

Arango, J.L. & Ponce, A. 1980. Memoria explicativa: Reseña explicativa del mapa geológico del departamento de Nariño. Scale 1:400 000. Ingeominas, 40 p. Bogotá.

Aspden, J. 1984. The geology of the Western Cordillera and Pacific coastal plain in the Department of Valle del Cauca (sheets 261, 278, 279, 280 and 299). Ingeominas–Misión Británica, Internal report 1959, 61 p. Cali.

Aspden, J. & Nivia, A. 1985. Memoria explicativa: Reseña explicativa del mapa geológico preliminar de la plancha 278 bahía de Buenaventura. Scale 1:100 000. Ingeominas, 13 p. Bogotá.

Aubry, M.P. 2014. Cenozoic coccolithophores: Discoasterales (CC–B). Atlas of micropaleontology series, part 1 of 4. The Micropaleontology Press Foundation, 104 p. New York.

Aubry, M. 2015. Cenozoic coccolithophores: Discoasterales (CC–D). Atlas of micropaleontology series. The Micropaleontology Press Foundation, 433 p. New York.

Backman, J., Raffi, I., Rio, D., Fornaciari, E. & Pälike, H. 2012. Biozonation and biochronology of Miocene through Pleistocene calcareous nannofossils from low and middle latitudes. Newsletters on Stratigraphy, 45(3): 221–244. https://doi.org/10.1127/0078-0421/2012/0022

Barbosa–Espitia, A.A., Restrepo–Moreno, S.A., Pardo–Trujillo, A., Osorio, J.A. & Ochoa, D. 2013a. Uplift and exhumation of the southernmost segment of the Western Cordillera, Colombia, and development of the neighboring Tumaco Basin. GSA Annual Meeting 125th Anniversary of GSA. Proceedings 45(7): p. 548. Denver, USA.

Barbosa–Espitia, A.A., Restrepo–Moreno, S., Pardo–Trujillo, A., Ochoa, D.I. & Osorio, J.A. 2013b. Uplift and exhumation of the southernmost segment of the Western Cordillera and development of the Tumaco Basin. XIV Congreso Colombiano de Geología. Abstract, p. 387. Medellín.

Barbosa–Espitia, A.A., Foster, D.A., Restrepo–Moreno, S.A., Pardo–Trujillo, A. & Kamenov, G. 2016. Geochemistry and geochronology of plutonic rocks from the Colombian Western Cordillera: New insights into the Cenozoic tectonics of the NW South American plate margin. GSA Annual Meeting. Abstracts with Programs, 48(7): Paper No. 347–27. https://doi.org/10.1130/abs/2016AM-279826

Barrero, D., Laverde, F., Ruiz, C.C. & Alfonso, C.A. 2006. Oblique collision and basin formation in western Colombia: The origin, evolution and petroleum potential of Cauca–Patía Basin. IX Simposio Bolivariano de Exploración en Cuencas Subandinas. Abstracts CD ROM. Cartagena, Colombia.

Barrero, D., Pardo, A., Vargas, C.A. & Martínez, J.F. 2007. Colombian sedimentary basins: Nomenclature, boundaries and petroleum geology, a new proposal. Agencia Nacional de Hidrocarburos, 92 p. Bogotá.

Bedoya, E.L., Flores, J.A. & Pardo, A. 2013. Nanofósiles calcáreos y bioestratigrafía del Mioceno tardío del SW de la Cuenca Tumaco onshore, Pacífico colombiano. Boletín de Geología, 35(1): 55–66.

Berggren, W.A., Kent, D.V., Swisher III, C.C. & Aubry, M.P. 1995. A revised Cenozoic geochronology and chronostratigraphy. In: Berggren, W.A., Kent, D.V., Aubry, M.P. & Hardenbol, J. (editors), Geochronology, time scales and global stratigraphic correlation. SEPM Special Publications 54: p. 129–212. https://doi.org/10.2110/pec.95.04.0129

Bermúdez, H.D., García, J., Stinnesbeck, W., Keller, G., Rodríguez, J.V., Hanel, M., Hopp, J., Schwarz, W., Trieloff, M., Bolívar, L. & Vega, F.J. 2016. The Cretaceous – Paleogene boundary at Gorgonilla Island, Colombia, South America. Terra Nova, 28(1): 83–90. https://doi.org/10.1111/ter.12196

Blow, W.H. 1969. Late middle Eocene to recent planktonic foraminiferal biostratigraphy. In: Bronnimann, P. & Renz, H.H. (editors), Proceedings of the First International Conference on Planktonic Microfossils, 1, p. 199–422. Geneva, Switzerland.

Borrero, C., Pardo, A., Jaramillo, C.M., Osorio, J.A., Cardona, A., Flores, A., Echeverri, S., Rosero, S., García, J. & Castillo, H. 2012. Tectonostratigraphy of the Cenozoic Tumaco Forearc Basin, Colombian Pacific, and its relationship with the northern Andes orogenic build up. Journal of South American Earth Sciences, 39: 75–92. https://doi.org/10.1016/j.jsames.2012.04.004

Cediel, F., Restrepo, I., Marín–Cerón, M.I., Duque–Caro, H., Cuartas, C., Mora, C., Montenegro, G., García, E., Tovar, D. & Muñoz, G. 2009. Geology and hydrocarbon potential, Atrato and San Juan Basins, Chocó (Panamá) Arc. Tumaco Basin (Pacific realm), Colombia. Agencia Nacional de Hidrocarburos and Fondo Editorial Universidad EAFIT, 172 p. Medellín, Colombia.

Cohen, K.M., Finney, S.C., Gibbard, P.L. & Fan, J.X. 2013 (updated 2017/02). The ICS International Chronostratigraphic Chart. Episodes, 36(3): 199–204.

Cortés, J.E., Mejía–Molina, A., Morton, A., Vargas, C.A. & Cortés, S.I. 2019. Provenance, tectonic setting, and weathering of sediments in Tumaco–1 ST–P well, Tumaco Forearc Basin, Colombia: Insights from petrography, heavy minerals, X–ray diffraction, and whole–rock chemostratigraphy. Journal of South American Earth Sciences, 96: 102219. https://doi.org/10.1016/j.jsames.2019.102219

Dickinson, W.R. & Gehrels, G.E. 2009. Use of U–Pb ages of detrital zircons to infer maximum depositional ages of strata: A test against a Colorado Plateau Mesozoic database. Earth and Planetary Science Letters, 288(1–2): 115–125. https://doi.org/10.1016/j.epsl.2009.09.013

Echeverri, S. 2012. Estratigrafía y análisis de procedencia del intervalo Eoceno – Plioceno de la cuenca de forearc de Tumaco "onshore" (SW de Colombia) y su relación con la tectónica de la margen pacífica del NW de Suramérica. Master thesis, Universidad de Caldas, 127 p. Manizales.

Echeverri, S., Borrero, C., Moreno, M., Pardo–Trujillo, A. & Castillo, H. 2011. Nomenclatura estratigráfica para la sucesión neógena expuesta en la bahía de Tumaco, Cuenca Tumaco costa adentro, SW de Colombia: Redefinición y formalización. XIV Congreso Latinoamericano de Geología y XIII Congreso Colombiano de Geología. Abstracts, p. 364. Medellín, Colombia.

Echeverri, S., Cardona, A., Pardo–Trujillo, A., Borrero, C., Rosero, S. & López, S. 2015a. Correlación y geocronología Ar–Ar del basamento cretácico y el relleno sedimentario Eoceno superior – Mioceno (Aquitaniano inferior) de la cuenca de antearco de Tumaco, SW de Colombia. Revista Mexicana de Ciencias Geológicas, 32(2): 179–189.

Echeverri, S., Cardona, A., Pardo, A., Mosalve, G., Valencia, V.A., Borrero, C., Rosero, S. & López, S. 2015b. Regional provenance from southwestern Colombia fore–arc and intra–arc basins: Implications for middle to late Miocene orogeny in the northern Andes. Terra Nova, 27(5): 356–363. https://doi.org/10.1111/ter.12167

Echeverri, S., Pardo–Trujillo, A., Borrero, C., Cardona, A., Rosero, S., Celis, S.A. & López, S.A. 2016. Estratigrafía del Neógeno superior al sur de la Cuenca Tumaco (Pacífico colombiano): La Formación Cascajal, propuesta de redefinición litoestratigráfica. Boletín de Geología, 38(4): 43–60. http://dx.doi.org/10.18273/revbol.v38n4-2016003

Escovar, R., Gómez, L.A. & Ramírez, J.R. 1992. Interpretación de la sísmica Tumaco 90 y evaluación preliminar del área: Bogotá. Empresa Colombiana de Petróleos, unpublished report, 74 p. Bogotá.

Folk, R. 1974. Petrology of sedimentary rocks. Hemphill Publishing Company, 182 p. Austin, USA.

García, J. 2012. Procedencia de los sedimentos neógenos de Tumaco onshore y Gorgona: Una contribución a la tectónica de antearco del Pacífico sur de Colombia. Master thesis, Universidad de Caldas, 82 p. Manizales, Colombia.

Gehrels, G.E., Valencia, V. & Pullen, A. 2006. Detrital zircon geochronology by laser–ablation multicollector ICPMS at the Arizona LaserChron Center. In: Loszewski, T. & Huff, W. (editors), Geochronology: Emerging opportunities. Paleontology Society Short Course: Paleontology Society Papers, 11, 10 p.

Giraldo–Villegas, C.A., Celis, S.A., Rodríguez–Tovar, F.J., Pardo–Trujillo, A., Vallejo–Hincapié, D.F. & Trejos–Tamayo, R.A. 2016. Ichnological analysis of the upper Miocene in the ANH–Tumaco–1–ST–P well: Assessing paleoenvironmental conditions at the Tumaco Basin, in the Colombian Pacific. Journal of South American Earth Sciences, 71: 41–53. https://doi.org/10.1016/j.jsames.2016.06.008

Gómez, J., Montes, N.E., Nivia, Á. & Diederix, H., compilers. 2015. Geological Map of Colombia 2015. Scale 1:1 000 000. Servicio Geológico Colombiano, 2 sheets. Bogotá. https://doi.org/10.32685/10.143.2015.936

González, H., compiler. 2008. Investigación integral del Andén Pacífico colombiano. Tomo 1: Geología; Cuenca de Tumaco. Igac–Ingeominas. p. 85–86. Bogotá.

Hall, M.L. & Wood, C.A. 1985. Volcano–tectonic segmentation of the northern Andes. Geology, 13(3): 203–207. https://doi.org/10.1130/0091-7613(1985)13<203:VSOTNA>2.0.CO;2

Haq, B.U., Hardenbol, J. & Vail, P.R. 1987. Chronology of fluctuating sea levels since the Triassic. Science, 235: 1156–1167.

Instituto Colombiano de Geología y Minería & Instituto Geográfico Agustín Codazzi. 2005. Mapa geológico de las planchas 361 Bis, 383 Tumaco, 384 La Chorrera, 407 Cabo Manglares y 408 Barbacoas. Scale 1:100 000. Bogotá.

Jaillard, E., Lapierre, H., Ordoñez, M., Toro–Álava, J., Amórtegui, A. & Vanmelle, J. 2009. Accreted oceanic terranes in Ecuador: Southern edge of the Caribbean Plate? Geological Society of

London, Special Publications 328, p. 469–485. https://doi.org/10.1144/SP328.19

Jaramillo, C., Rueda, M. & Torres, V. 2011. A palynological zonation for the Cenozoic of the Llanos and Llanos Foothills of Colombia. Palynology, 35(1): 46–84. https://doi.org/10.1080/01916122.2010.515069

Kennett, J.P. & Srinivasan, M.S. 1983. Neogene planktonic foraminifera: A phylogenetic atlas. Hutchinson Ross Publishing Company. 265 p.

Kochelek, E.J., Amato, J.M., Pavlis, T.L. & Clift, P.D. 2011. Flysch deposition and preservation of coherent bedding in an accretionary complex: Detrital zircon 111 ages from the Upper Cretaceous Valdez Group, Chugach Terrane, Alaska. Lithosphere, 3(4): 265–274.

León, L.A., Padilla, L.E. & Marulanda, N. 1973. Geología, recursos minerales y geoquímica de la parte NE del cuadrángulo 0–5 El Bordo, departamento del Cauca. Ingeominas, Internal report 1652, 235 p. Popayán.

López, P.A., Pardo, A., Ochoa, D. & Rosero, S. 2012. Palinología de los sedimentos recientes del río Mira, Pacífico colombiano. Geología Colombiana, 37(1): 21–22.

López–Ramos, E. 2009. Evolution tectono–stratigraphique du doble basin avant–arc de la marge convergente Sud Colombienne–Nord Equatorienne pedant le Cenozoïque. Doctorade thesis, Université de Nice Sophia Antipolis, 349 p. Nice, France.

Lourens, L.J., Hilgen, F.J., Shackleton, N.J., Laskar, J. & Wilson, D. 2004. The Neogene Period. In: Gradstein, F.M., Ogg, J.G. & Smith, A.G. (editors), Geological time scale 2004, Cambridge University Press, pp. 409–440. Cambridge, UK.

Ludwing, K.R. 2003. User´s manual for Isoplot 3.00: A geochronological toolkit for Microsoft Excel. Berkeley Geochronology Center, Special Publication (4), 70 p.

Mange, M.A. & Maurer, H.F.W. 1992. Heavy minerals in colour. Chapman & Hall, 147 p. London, UK.

Marcaillou, B. & Collot, J.Y. 2008. Chronostratigraphy and tectonic deformation of the north Ecuadorian–South Colombian offshore Manglares Forearc Basin. Marine Geology, 255(1–2): 30–44. https://doi.org/10.1016/j.margeo.2008.07.003

Marín–Cerón, M.I. & Sierra, G. 2011. Tumaco Basin. In: Cediel, F. (editor), Petroleum geology of Colombia: Geology and hydrocarbon potential, 13. Agencia Nacional de Hidrocarburos and Universidad EAFIT, 77 p. Medellín.

Martini, E. 1971. Standard Tertiary and Quaternary calcareous nannoplankton zonation. Proceedings 2nd Planktonic Conference, Proceedings, 739–785. Roma, Italy.

Moreno–Sánchez, M. & Pardo–Trujillo, A. 2003. Stratigraphical and sedimentological constraints on western Colombia: Implications on the evolution of the Caribbean Plate. In: Bartolini, C., Buffler, R.T. & Blickwede, J. (editors), The circum–Gulf of Mexico and the Caribbean: Hydrocarbon habitats, basin formation, and plate tectonics. American Association of Petroleum Geologists Memoir 79, p. 891–924. Tulsa, USA.

Nelson, H.W. 1962. Contribución al conocimiento de la cordillera Occidental: Sección carretera Cali–Buenaventura. Boletín Geológico, 10(1–3): 81–108.

Nivia, A., Pérez, C. & Sepúlveda, J. 2003. Memoria explicativa: Geomorfología y geología de la plancha 383 Tumaco. Scale: 1:100 000. Ingeominas, 39 p. Cali, Colombia.

Okada, H. & Bukry, D. 1980. Supplementary modification and introduction of code numbers to the low–latitude coccolith biostratigraphic zonation (Bukry, 1973; 1975). Marine Micropaleontology, 5: 321–325. https://doi.org/10.1016/0377-8398(80)90016-X

Oppenheim, V. 1949. Geología de la costa sur del Pacífico de Colombia. Boletín Instituto Geofísico de los Andes Colombianos, (1), Serie C: 4–23.

Pardo–Casas, F. & Molnar, P. 1987. Relative motion of the Nazca (Farallon) and South American Plates since Late Cretaceous time. Tectonics, 6(3): 233–248. https://doi.org/10.1029/TC006i003p00233

Perch–Nielsen, K. 1985. Mesozoic calcareous nannofossils. In: Bolli, H., Saunders, J.B. & Perch–Nielsen, K. (editors), Plankton stratigraphy. Cambridge University Press, p. 329–426.

Pindell, J.L. & Kennan, L. 2009. Tectonic evolution of the Gulf of Mexico, Caribbean and northern South America in the mantle reference frame: An update. In: James, K.H., Lorente, M.A. & Pindell, J.L. (editors), The origin and evolution of the Caribbean Plate. Geological Society of London, Special Publication 328, p. 1–55. https://doi.org/10.1144/SP328.1

Raffi, I., Backman, J., Fornaciari, E., Pälike, H., Rio, D., Lourens, L. & Hilgen, F. 2006. A review of calcareous nannofossil astrobiochronology encompassing the past 25 million years. Quaternary Science Reviews, 25(23–24): 3113–3137. https://doi.org/10.1016/j.quascirev.2006.07.007

Ramos, V.A. 1999. Plate tectonic setting of the Andean Cordillera. Episodes, 22(3): 183–190.

Robertson Research inc. & Empresa Colombiana de Petróleos. 1981a. Geochemical and biostratigraphic analysis of Wainoco No.1, Majagua, Colombia. Internal report 413, 61 p. Houston, USA.

Robertson Research inc. & Empresa Colombiana de Petróleos. 1981b. Biostratigraphic, geochemical and petrological analysis of samples from Arco well Remolino Grande–1, Colombia. Internal report 318, 75 p. Houston, USA.

Serrano, L., Ferrari, L., López–Martínez, M., Petrone, C.M. & Jaramillo, C. 2011. An integrative geologic, geochronologic and geochemical study of Gorgona Island, Colombia: Implications for the formation of the Caribbean Large Igneous Province. Earth and Planetary Science Letters, 309(3–4): 324–336. https://doi.org/10.1016/j.epsl.2011.07.011

Somoza, R. 1998. Updated Nazca (Farallon)–South America relative motions during the last 40 My: Implications for mountain building in the central Andean region. Journal of South American Earth Sciences, 11(3): 211–215. https://doi.org/10.1016/S0895-9811(98)00012-1

Somoza, R. & Ghidella, M.E. 2012. Late Cretaceous to recent plate motions in western South America revisited. Earth and Planetary Science Letters, 331–332: 152–163. https://doi.org/10.1016/j.epsl.2012.03.003

Spadea, P. & Espinosa, A. 1996. Petrology and chemistry of Late Cretaceous volcanic rocks from the southernmost segment of the Western Cordillera of Colombia (South America). Journal of South American Earth Sciences, 9(1–2): 79–90. https://doi.org/10.1016/0895-9811(96)00029-6

Spikings, R. & Crowhurst, P. 2004. (U–Th)/He thermochronometric constraints on the late Miocene – Pliocene tectonic development of the northern Cordillera Real and the Interandean Depression, Ecuador. Journal of South American Earth Sciences, 17: 239–251.

Spikings, R.A. & Simpson, G. 2014. Rock uplift and exhumation of continental margins by the collision, accretion, and subduction of buoyant and topographically prominent oceanic crust. Tectonics, 33(5): 635–655. https://doi.org/10.1002/2013TC003425

Spikings, R.A., Winkler, W., Hughes, R.A. & Handler, R. 2005. Thermochronology of allochthonous terranes in Ecuador: Unravelling the accretionary and post–accretionary history of the northern Andes. Tectonophysics, 399(1–4): 195–220.

Spikings, R., Crowhurst, P.V., Winkler, W. & Villagómez, D. 2010. Syn– and post–accretionary cooling history of the Ecuadorian Andes constrained by their in–situ and detrital thermochronometric record. Journal of South American Earth Sciences, 30(3–4): 121–133. https://doi.org/10.1016/j.jsames.2010.04.002

Suárez, M.A. 1990. Estudio geológico regional e interpretación sísmica estratigráfica en la provincia sedimentaria de la costa Pacífica. Ecopetrol, unpublished report, 119 p. Bogotá.

Suárez, M.A. 2007. Geological framework of the Pacific coast sedimentary basins. Geología Colombiana, 32: 47–62.

Vallejo, C., Winkler, W., Spikings, R.A., Luzieux, L., Heller, F. & Bussy, F. 2009. Mode and timing of terrane accretion in the forearc of the Andes in Ecuador. In: Kay, S.M., Ramos, V.A. & Dickinson, W.R. (editors), Backbone of the Americas: Shallow subduction, plateau uplift, and ridge and terrane collision. Geological Society of America, Memoirs 204, p. 197–216. https://doi.org/10.1130/2009.1204(09)

van der Hammen, T. 1958. Estratigrafía del Terciario y Maastrichtiano continentales y tectogénesis de los Andes colombianos. Boletín Geológico, 6(1–3): 67–128.

van der Hammen, T., Werner, J.H. & van Dommelen, H. 1973. Palynological record of the upheaval of the northern Andes: A study of the Pliocene and lower Quaternary of the Colombian Eastern Cordillera and the early evolution of its high–Andean biota. Review of Palaeobotany and Palynology, 16(1–2): 1–122. https://doi.org/10.1016/0034-6667(73)90031-6

Villagómez, D., Spikings, R., Magna, T., Kammer, A., Winkler, W. & Beltrán, A. 2011. Geochronology, geochemistry and tectonic evolution of the Western and Central Cordilleras of Colombia. Lithos, 125(3–4): 875–896. https://doi.org/10.1016/j.lithos.2011.05.003

Wade, B.S., Pearson, P.N., Berggren, W.A. & Pälike, H. 2011. Review and revision of Cenozoic tropical planktonic foraminiferal biostratigraphy and calibration to the geomagnetic polarity and astronomical time scale. Earth–Science Reviews, 104(1–3): 111–142. https://doi.org/10.1016/j.earscirev.2010.09.003

Explanation of Acronyms, Abbreviations, and Symbols:

ANH	Agencia Nacional de Hidrocarburos
AP–T	Andrés Pardo–Trujillo
FAD	First Appearance Datum
LA–ICPMS	Laser ablation inductively coupled plasma mass spectrometry
TD	Total depth

Authors' Biographical Notes

Andrés PARDO–TRUJILLO is a geologist in the Departamento de Ciencias Geológicas at the Universidad de Caldas (Manizales, 1998). Andres obtained his MS in vegetal micropaleontology in 1997 and his PhD in Science from Liège University (Belgium, 2004). He has worked since 1989 as a professor in the Departamento de Ciencias Geológicas at Universidad de Caldas, Colombia, in sedimentology, regional geology, palynology, and field geology. From 2006–2009, he worked as an advisor at the Agencia Nacional de Hidrocarburos (ANH), where he participated in the geological study of several Colombian sedimentary basins. Andres is currently the director of the Instituto de Investigaciones en Estratigrafía (IIES) and of the Grupo de Investigación en Estratigrafía y Vulcanología (GIEV) at the Universidad de Caldas. His main interest is the study of the geological and biological evolution of the NW corner of South America during the Cretaceous – Cenozoic.

Sebastián ECHEVERRI is a geologist from the Universidad de Caldas (Colombia), with an MS in earth sciences from the same university and a PhD in science–geotectonics from the Universidade de São Paulo (Brasil). Sebastián works as a researcher in the Grupo de Investigación en Estratigrafía y Vulcanología (GIEV) Cumanday – Instituto de Investigaciones en Estratigrafía (IIES) at Universidad de Caldas (Colombia) and is part of the EGEO research group of the Universidad Nacional (Medellín). His main research area is the regional geology and tectono–stratigraphic evolution of convergent margins.

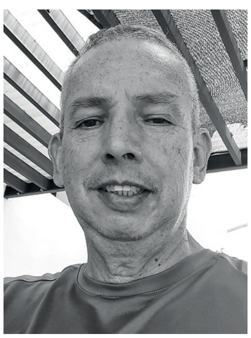

Carlos BORRERO attained a BS in geology from Universidad Nacional de Colombia (Bogotá, 1983). Stratigraphy, volcanology, field geology, and hazard and risk assessment and management have been the focus of his long career in academia at Universidad de Caldas (Manizales, 1985–2015) and as a consultant geologist (1991–present). Currently, he is semiretired.

Alejandro ARENAS is a geologist of the Departamento de Ciencias Geológicas at the Universidad de Caldas (Manizales, Colombia) and has an MS in earth sciences from the Universidad de Caldas (Manizales, Colombia). Alejandro has worked in REDCOM as a professional for Ecopetrol in the field of reservoir development. Alejandro is currently a researcher at the Instituto de Investigaciones en Estratigrafía (IIES) and belongs to the Grupo de Investigación en Estratigrafía y Vulcanología (GIEV) Cumanday. He has strong capabilities in 3D modeling and seismic interpretation.

Felipe VALLEJO is a geologist from the Universidad de Caldas (Colombia), MS and PhD student in geology at Universidad de Salamanca (Spain). Felipe works as a researcher and consultant at the Instituto de Investigaciones en Estratigrafía (IIES) of the Universidad de Caldas (Colombia). Felipe is also part of the Grupo de Investigación en Estratigrafía y Vulcanología (GIEV) Cumanday. His work has been focused on building a biostratigraphic and biochronologic framework based on calcareous nannofossils for the Caribbean and Pacific Basins of Colombia.

Raúl TREJOS is a geologist from the Universidad de Caldas (Colombia) and has an MS in earth sciences from the Universidad de Salamanca (Spain). He is currently a PhD student in geology at the Universidad de Salamanca. Since 2013, Raúl has worked as a researcher at the Instituto de Investigaciones en Estratigrafía (IIES) – Universidad de Caldas and belongs to the Grupo de Investigación en Estratigrafía y Vulcanología (GIEV) Cumanday. He is recognized as a junior researcher by the Ministerio de Ciencias, Tecnología e Innovación in Colombia. His main experience is in micropaleontology (foraminifera).

Ángelo PLATA obtained his bachelor's degree in biology from the Universidad Industrial de Santander, Colombia, in 2007. He worked at the Colombian oil company Ecopetrol for 5 years as a junior biostratigrapher before going to Spain in 2012 to obtain his Master of Earth Science degree from the Department of Geology, Universidad de Salamanca. After returning from Universidad de Salamanca, he began his current role as palynologist in chief of the Palynology Lab for Instituto de Investigaciones en Estratigrafía, Universidad de Caldas, where he studies terrestrial palynomorphs and marine diatoms. Currently, Angelo is a candidate for his PhD at Universidad de Salamanca.

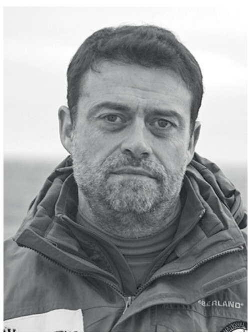

José–Abel FLORES is a geologist in the Department of Geology of the Universidad de Salamanca (Spain) and obtained his PhD in sciences at the Universidad de Salamanca in 1997. A specialist in calcareous nannofossils, he has been a full professor of micropaleontology and oceanography since 2006 and an invited professor in several institutions in Europe, the Americas, and Japan. He centered his research in biostratigraphy and paleoceanography, participating in five ODP/IOPD expeditions and working with different hydrocarbon companies (Repsol, Gas Natural, Petrobras, Ecopetrol, Exxon). His interest and expertise cover the Cretaceous to present–day environments, combining microfossil and biogeochemistry information. In recent years, he has participated in several Colombian projects with the Universidad de Caldas, particularly the paleoceanographic evolution of tertiary basins, the consequences of the communication between the Atlantic and the Pacific, and the definition of a high–resolution astronomically calibrated scale based on micro and calcareous nannofossils.

Agustín CARDONA is graduated with a degree in geology from Universidad EAFIT in 1999. He obtained MS and PhD degrees in geochemistry and geotectonics, respectively, from the Universidade de São Paulo, Brasil. Subsequently, he was a postdoctoral fellow at the Smithsonian Tropical Research Institute (2006–2011), working in several paleogeogeographic–oriented projects in northern Colombia and Panamá. Since 2012, he has served as full–time professor at the Universidad Nacional de Colombia in Medellín. His main interest is related to regional tectonics of convergent margins, especially the Andean and Caribbean Orogens.

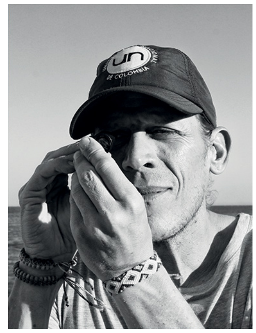

Sergio RESTREPO is a geologist from Universidad Nacional de Colombia. He holds a PhD in geology and geography from the Department of Geological Sciences at the University of Florida (UF, 2009) and is currently an associate professor in the Departamento de Geociencias y Medio Ambiente at Universidad Nacional de Colombia and adjunct postdoctoral researcher at University of Florida. Sergio completed two postdoctoral studies under the auspices of the Smithsonian Institution (2009–2010) and the National Science Foundation (2011). During his doctoral and postdoctoral work, Sergio received research support from GSA, AGI, NSF, and the COMPTON Foundation, among others. Since 2010, Sergio has collaborated in several interdisciplinary projects carried out by the Instituto de Investigaciones en Estratigrafía (Universidad de Caldas, Colombia) while also developing some investigations supported by Colciencias and the National Geographic Society. Sergio's work in geosciences concentrates on the use of geochronology, thermochronology, and isotopic tools to understanding morphotectonic process over various spatio-temporal scales, as well as on the development of educational tools to advance earth and environmental literacy among rural communities. Geographically, Sergio's work focuses on the Andes, the Caribbean, and Central America.

Ángel BARBOSA is a Colombian geologist who obtained his bachelor's degree from the Universidad de Caldas in 2009 and an MS in geological sciences in 2012. His master's thesis focused on low–temperature thermochronology applied to understand the thermotectonic coevolution of the south part of the Colombian Western Cordillera and the Tumaco Basin. He has worked on several projects in Colombia involving geological mapping, sampling, and the use of analytic techniques such as mass spectrometry to obtain thermo and geochronologic data. Angel is currently a PhD candidate at the University of Florida, where he has served as a TA, teaching several courses, including physical geology, engineering and environmental geology, and introduction to earth science. His research interests include understanding the Cenozoic tectonic evolution of the NW Andes using the magmatic and sedimentary record within sedimentary basins and cordilleran massifs and investigating the role of sediments in the origin and evolution of continental crust.

Hugo MURCIA is a geologist from the Universidad de Caldas, Colombia, who received his MS in earth sciences from the Universidad Nacional Autónoma de México, México, and his PhD in geology from the University of Auckland, New Zealand. Hugo works as a professor at the Departamento de Ciencias Geológicas as a researcher at the Instituto de Investigaciones en Estratigrafía (IIES), both at Universidad de Caldas, Colombia. Hugo also belongs to the Grupo de Investigación en Estratigrafía y Vulcanología (GIEV) Cumanday and is recognized as an associate researcher by the Ministerio de Ciencias, Tecnología e Innovación in Colombia. He specializes in volcanology and petrology.

Carlos GIRALDO is a geologist of the Departamento de Ciencias Geológicas de la Universidad de Caldas (Manizales, Colombia, 2014) and a student of the Master of Earth Sciences program at the Universidad de Caldas. During 2014–2015, he worked at the Instituto de Investigaciones Marinas y Costeras José Benito Vives de Andréis (INVEMAR) in areas related to marine geology. Since 2015, he has been linked to the Instituto de Investigaciones en Estratigrafía (IIES) and the Grupo de Investigación en Estratigrafía y Vulcanología (GIEV) Cumanday. His research field is related to ichnology, sedimentology, and stratigraphy, and its integration into sedimentary basin analysis to reconstruct ancient depositional environments and interpret their possible sequence stratigraphic framework.

Sergio CELIS is a geologist from the Universidad de Caldas (Colombia), has an MS in earth sciences from the same university, and received his PhD in earth sciences from the University of Granada (Spain). Sergio is a researcher at the Instituto de Investigaciones en Estratigrafía (IIES) and has experience as a professor in the Departamento de Ciencias Geológicas at the Universidad de Caldas. Sergio also belongs to the Grupo de Investigación en Estratigrafía y Vulcanología (GIEV) Cumanday and is recognized as a junior researcher by the Ministerio de Ciencias, Tecnología e Innovación in Colombia. His main experience is in ichnology and basin analysis.

Sergio A. LÓPEZ is graduated with a bachelor's degree in geology from the Universidad de Caldas, Colombia, and received a master's degree in earth and environmental sciences from the Universidad EAFIT, Medellín, Colombia, with an emphasis on morphodynamics of tropical deltaic systems. He currently holds a doctoral candidate position in the Department of Geological Sciences from the Universidad de Buenos Aires, Argentina. He has worked as a researcher in interdisciplinary projects on modern deltas (Universidad EAFIT, 2004–2008), active tectonics and geodynamics (Servicio Geológico Colombiano, 2008–2010), and as advisor of the new ventures technical team from the Agencia Nacional de Hidrocarburos (2011–2017).